Disturbance Reduction in Nonlinear Sytems via Adaptive Quenching

by

Bryan Dwayne Heydon

Thesis submitted to the Faculty of the

Virginia Polytechnic Institute and State University

in partial fulfillment of the requirements for the degree of

Master of Science

in

Electrical Engineering

APPROVED:

Dr. A. H. Nayfeh, Co-chairperson

Dr. W. T. Baumann, Co-chairperson

Dr. H. F. VanLandingham

May, 1990

Blacksburg, Virginia

Disturbance Reduction in Nonlinear Sytems via Adaptive Quenching

by

Bryan Dwayne Heydon

Dr. A. H. Nayfeh, Co-chairperson

Dr. W. T. Baumann, Co-chairperson

Electrical Engineering

(ABSTRACT)

Abstract

An indirect adaptive quenching algorithm for a nonlinear single-degree-of-freedom system with unknown constant system parameters is presented. The system is subject to external or parametric sinusoidal disturbances and the resulting control signal is also sinusoidal. The quenching algorithm provides a reduction in the control effort required compared to direct disturbance cancellation. The disturbance sinusoid and the unknown parameters are incorporated into the system model and an extended Kalman filter (EKF) with modified update equations is used to estimate the system state and parameters. The estimates are then used to form the quenching signal. The adaptive quenching algorithm is found to work well inside a quenching region defined by the separatrices and suggests the

use of a hybrid control law. The algorithm was verified by implementing it on an analog computer.

Acknowledgements

I would like to express my sincere appreciation and thanks to Dr. A. H. Nayfeh for his support and guidance which made my thesis work a pleasurable and enlightening experience. I have benefited greatly from his association and I hope to have the opportunity to work with him again in the future.

Dr. W. T. Baumann deserves special thanks for the numerous brain storming sessions we had in his office. He always had a free minute to discuss my work and his consideration is greatly appreciated.

I would like to thank Dr. H. F. VanLandingham for his time and effort on the behalf of my thesis.

This work was supported by the Army Research Office under Grant No. DAAL03-89-K-0180 and the Office of Naval Research under Grant No. N000014-83-K-0184, NR4322753, and Grant No. N00014-90-J-1149.

Finally, I thank Mrs. Sally Shrader who proved to be a wonderful source of information and relieved me from much of the paperwork associated with being a graduate student.

I dedicate this thesis to my parents, Craig and Mary Heydon, whose constant encouragement throughout my academic career made my thesis possible.

Table of Contents

List of Illustrations

CHAPTER 1

INTRODUCTION

1.1 Preview

In many realistic control problems, the system to be controlled is subjected to persistently acting external disturbances which are not known beforehand. If nothing is known about the form of the disturbance, it is usually modeled as noise and the resulting controller or regulator design tries to minimize the variance of the system output. If enough is known about the structure of the disturbance to model it by a set of differential equations, the disturbance can be incorporated into the system. Since the disturbance is unknown, controllers that incorporate the disturbance usually require some form of estimator.

This thesis is concerned with reducing the effect of resonant sinusoidal disturbances on the response of a nonlinear system with unknown constant parameters. The reduction is accomplished by introducing a second resonant excitation referred to as a quenching signal. Since the disturbance and system parameters are assumed to be unknown, the quenching algorithm will be implemented adaptively using a modified extended Kalman filter.

1.2 Literature review

Let us define the regulation problem as that of controlling a fixed plant to track a given reference signal while rejecting a disturbance signal generated by a dynamical system external to the plant. Hepburn and Wonham [1], Francis and Wonham [2], and Francis, Sebakhy and Wonham [3] have shown using a geometrical approach that a compensator which satisfies the regulation problem must incorporate a 'copy' or internal model of the disturbance dynamics along with the reference dynamics. The system can be augmented to include the deterministically modeled disturbance as an uncontrollable mode of the expanded system. The problem is then to design a feedback compensator which renders the uncontrollable mode unobservable at the output of the system. Chalam [4] discusses an algorithm proposed by Elliott and Goodwin [5] for discrete-time adaptive pole placement incorporating the internal model principle. Palaniswami and Goodwin [6] improved the

algorithm by reducing the number of parameters to be estimated. The internal model principle has been extended to nonlinear systems by Benedetto [7]. A geometrical approach was again used to prove the existence and form of the internal model needed for regulation but no practical implementation procedure was given.

Quenching is a phenomenon in nonlinear systems that results from the interaction of two different resonant excitations. The quenching or reduction of the response of a nonlinear system has been investigated for several systems subjected to sinusoidal excitations. In [8], Nayfeh analyzed the response of a bowed structure modeled by a pair of coupled second-order nonlinear differential equations to two external harmonic excitations. He was concerned with combination resonances and showed that if certain conditions concerning the amplitudes and the phase angle between the two excitations were satisfied, the response would be quenched and consist of essentially the linear response. Plaut, HaQuang, and Mook [9] investigated a system of nonlinear equations which model structural elements having curvature and exhibiting mid-surface stretching during motion. They showed that quenching is possible for certain cases of simultaneous primary and superharmonic resonant excitations. In a series of three articles, Nayfeh studied the response of a single-degree-of-freedom system with quadratic and cubic nonlinearities. Quenching was found to occur under certain conditions of excitation amplitude, frequency, and phase for the cases of simultaneous primary and superharmonic resonances [10], primary and combination resonances of the

additive or difference type [11], and principal parametric and subharmonic resonances [12].

Quenching should not be confused with the use of dither signals in nonlinear systems. Typically a dither is a much higher frequency signal than the system cutoff frequency and therefore is greatly attenuated before reaching the output. A dither signal [13] is introduced into a nonlinear system to augment stability or eliminate undesirable jump-phenomena and not necessarily to reduce the system response.

1.3 Organization of Thesis

An adaptive pole placement algorithm incorporating the internal model principle [4,6] is reviewed in Chapter 2. Insights from the algorithm provide the basis of comparison for the quenching algorithm. In Chapter 3 the deterministic quenching algorithm is presented for a single-degree-of-freedom system with quadratic and cubic nonlinearities. The quenching requirements are given for the parametric and subharmonic resonant cases [12] and the primary and superharmonic resonant cases [10]. Numerical examples are used to demonstrate the sensitivity of the quenching algorithm to variations in the quenching requirements. Chapter 4 begins by giving the equations of the modified EKF used to estimate the unknown disturbance and system parameters. The performance of the filter is discussed and the effect of initial

conditions on the adaptive quenching algorithm is investigated. The chapter concludes with an analog-computer verification of the adaptive algorithm using a digital-computer interface. Finally, Chapter 5 contains conclusions and some ideas for future research.

CHAPTER 2

THE INTERNAL MODEL PRINCIPLE

2.1 Regulation Using the Internal Model Principle

We consider an unknown linear time-invariant plant subject to unknown but deterministically modeled disturbances as shown in Figure 1. The input/output relationship of the plant is given by the autoregressive multivariate average (ARMA) difference equation

$$\tilde{A}(q^{-1})\tilde{y}(t) = \tilde{B}(q^{-1})\tilde{u}(t)$$

where $\tilde{A}(0) = 1, \tilde{B}(0) = 0, \tilde{n} = \max(\deg(\tilde{A}), \deg(\tilde{B}))$, and q^{-1} is the backward shift operator [14]. The shift operator is defined by

$$q^{-1}y(t) \triangleq y(t-1) \quad \text{for } t \geq 1; \quad q^{-1}y(0) \triangleq 0$$

and is used to write the difference equation in the time domain while the complex variable z from the z-transform is used in the frequency domain representation of the difference equation. It is analogous to the notational separation in continuous systems of the complex variable s in the Laplace transform and the differential operator $p = d/dt$. The disturbances can similarly be modeled as solutions to the homogeneous difference equations

$$D_i(q^{-1})d_i(t) = 0$$

$$D_0(q^{-1})d_0(t) = 0$$

$$D(q^{-1}) \equiv D_i(q^{-1})D_0(q^{-1})$$

where $D_i(0) = D_0(0) = 1$, $\deg(D_i) = n_i$, and $\deg(D_0) = n_0$. The following assumptions are needed:

i) $\tilde{n}$, n_i, and n_0 are known while the coefficients of $\tilde{A}$, $\tilde{B}$, D_i, and D_0 are unknown.
ii) The roots of D_i and D_0 are distinct and lie on the unit circle corresponding to bounded and nondiminishing disturbances.
iii) The polynomial pairs $(\tilde{A}D_i, \tilde{B}D_0)$ and $(\tilde{B}, D_0)$ are relatively prime.

From Figure 1 and the previous development, it can be shown that

$$A(q^{-1})y(t) = B(q^{-1})u(t) \tag{2.1}$$

where

$$A(q^{-1}) = \tilde{A}(q^{-1})D(q^{-1}) \tag{2.2}$$

$$B(q^{-1}) = \tilde{B}(q^{-1})D(q^{-1}) \tag{2.3}$$

$$n = \max(\deg(A), \deg(B)) = \tilde{n} + n_i + n_0.$$

Equation (2.1) is a higher-order ARMA model relating the controllable input and the measurable output with common factors in the A and B polynomials. The signals u(t) and y(t) are precisely the quantities required later for parameter estimation. From Figure 1 the control law can be written as

$$L(q^{-1})R(q^{-1})D(q^{-1})u(t) = P(q^{-1})[r(t) - y(t)] \tag{2.4}$$

where the compensator polynomials $P(q^{-1})$ and $L(q^{-1})$ satisfy the diophantine equation

$$L(q^{-1})R(q^{-1})D(q^{-1})\tilde{A}(q^{-1}) + P(q^{-1})\tilde{B}(q^{-1}) = A_d(q^{-1}) \tag{2.5}$$

The polynomial A_d is chosen to be stable with the desired closed loop poles. The polynomial $R(q^{-1})$ is known and satisfies the difference equation

$$R(q^{-1})r(t) = 0, \quad \deg(R) = n_r$$

where r(t) represents the reference signal to be tracked. To ensure a solution to equation (2.5) for arbitrary A_d, we assume that the polynomials $RD\tilde{A}$ and $\tilde{B}$ are relatively prime. Using the control law (2.4), we can write the closed loop system as

$$A_d(q^{-1})y(t) = P(q^{-1})\tilde{B}(q^{-1})r(t)$$

which shows that the disturbance will be unobservable at the output and that the output will track the reference signal asymptotically.

2.2 Adaptive Regulation

To implement the algorithm adaptively, we use a two-time-scale technique. During the time interval $t \in [kN,(k+1)N-1]$, a sequential least-squares algorithm with covariance reset is used to obtain estimates of A and B from which estimates of $\tilde{A}$, $\tilde{B}$, and D are derived. At each t = kN the diophantine equation (2.5) is resolved for new L and P polynomials. The time interval should satisfy the relationship $N \geq (3n + 2n_r)$.

If the ARMA model given in equation (2.1) is expanded, it can be rewritten in regression form as

$$y(t) = \phi(t-1)^T\theta_0$$

$$\theta_0 = [-a_1, ..., -a_n, b_1, ..., b_n]^T$$

$$\phi(t-1) = [y(t-1), ..., y(t-n), u(t-1), ..., u(t-n)]^T$$

where

$$A(q^{-1}) = 1 + \sum_{i=1}^{n} a_i q^{-i}$$

$$B(q^{-1}) = \sum_{i=1}^{n} b_i q^{-i}$$

The least-squares estimator is then given by

$$\hat{\theta}(t) = \hat{\theta}(t-1) + \frac{P(t-2)\phi(t-1)e(t)}{1 + \phi(t-1)^T P(t-2)\phi(t-1)}$$

$$P(t-1) = \begin{cases} P(t-1) - \dfrac{P(t-2)\phi(t-1)\phi(t-1)^T P(t-2)}{1 + \phi(t-1)^T P(t-2)\phi(t-1)}, & t \neq kN \\ \sigma_0 I, \quad t = kN \end{cases}$$

$$e(t) = y(t) - \phi(t-1)^T \hat{\theta}(t-1)$$

Using equations (2.2) and (2.3), we can write

$$\tilde{B}(q^{-1})\tilde{A}(q^{-1})D(q^{-1}) = \tilde{B}(q^{-1})A(q^{-1}) = B(q^{-1})\tilde{A}(q^{-1})$$

or

$$\tilde{A}(q^{-1})B(q^{-1}) - \tilde{B}(q^{-1})A(q^{-1}) = 0$$

Using the fact that $\tilde{A}(0) = 1$, we can rewrite the previous equation as

$$[\tilde{A}(q^{-1}) - 1]B(q^{-1}) - \tilde{B}(q^{-1})A(q^{-1}) = -B(q^{-1})$$

The estimates of $\tilde{A}$ and $\tilde{B}$ are obtained by equating the coefficients of like powers of q^{-1} and solving the resulting system of 2n equations for the $2\tilde{n}$ unknown coefficients of $\tilde{A}$ and $\tilde{B}$ using a pseudo left inverse. A similar technique is used to find $D(q^{-1})$. If the coefficients of like powers of q^{-1} in equations (2.2) and (2.3) are equated, the resulting system of 2n equations can be solved for the $(n_i + n_0)$ unknown coefficients of $D(q^{-1})$ using a pseudo left inverse. Using the estimates of A and $\tilde{B}$, equation (2.5) can be solved for P and L by again equating like powers of q^{-1}. To ensure solutions for P and L, we assume the degree of A_d to be $(2n + n_r - 1)$ or less and the degree of L and P to be $(n + n_r - 1)$. With the polynomials L, P, and D held fixed, the control signal u(t) is generated using equation (2.4) until the beginning of the next time interval N at which time the above process is repeated.

Remark 1: During estimation the polynomials $RD\tilde{A}$ and $\tilde{B}$ may share a common factor which will lead to ill-conditioning of the matrix involved in solving equation (2.5). If this happens, we just use the previous values of P and L for the next time interval N.

Remark 2: To ensure persistency of excitation and therefore convergence of the least-squares algorithm, we must not allow the norm of the coefficients associated with the polynomial $P(q^{-1})$ to fall below a given bound. If this

happens, the previous values of P and L are used again for the next time interval N.

2.3 Example

The input disturbance is given by $d_i(t) = c_1 \sin(2\pi t/T_d)$ where T_d is the period of the sinusoid in samples. The output disturbance will be assumed to be zero resulting in the disturbance model

$$D(q^{-1}) = 1 + d_1 q^{-1} + q^{-2}$$

The discrete time model of the plant was selected to be

$$H(q^{-1}) = \frac{0.48q^{-1} - 0.16q^{-2}}{1 - 1.8q^{-1} - 0.84q^{-2}}$$

The intermittent disturbance with an amplitude of $c_1 = 0.2$ and a period of $T_d = 18$ samples disappears every 270 samples. The reference signal was a square wave of period 220 samples. The control law was updated and the estimator gain was reset to $\sigma_0 = 5000$ every N = 18 samples. The desired closed loop poles are given by

$$A_d(q^{-1}) = 1 - 1.039q^{-1} + 0.36q^{-2}$$

corresponding to a 2% settling time of 8 samples and a percent overshoot of 4.6%. The tracking performance and disturbance regulation is shown in Figure 2. Except in the transient stage where the estimator is trying to find a good estimate of the plant, the algorithm works quite well. Figure 3 again shows the reference and disturbance signals along with the control input. Since superposition holds in linear systems, the control signal after each transient is just the constant value needed to obtain the reference step minus the disturbance. In the next chapter this will be referred to as direct disturbance cancellation. As an alternative to this method, the disturbance and the unknown plant coefficients could have been incorporated into the system using a state space representation and the augmented system estimated using a pseudo-linear parameter identification algorithm [15]. The same control signal as in Figure 3 could then have been computed from the estimates.

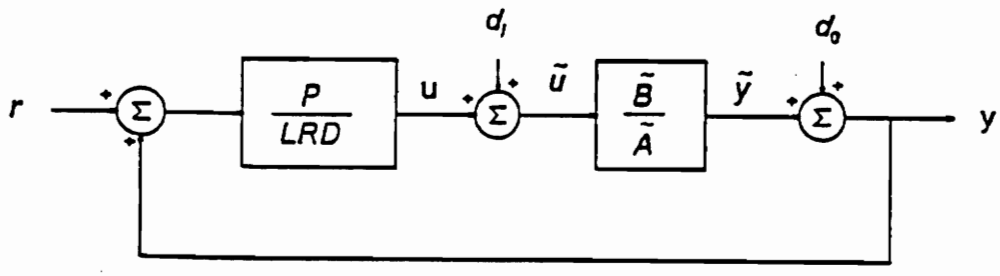

Figure 1. Adaptive Implementation of the Internal Model Principle

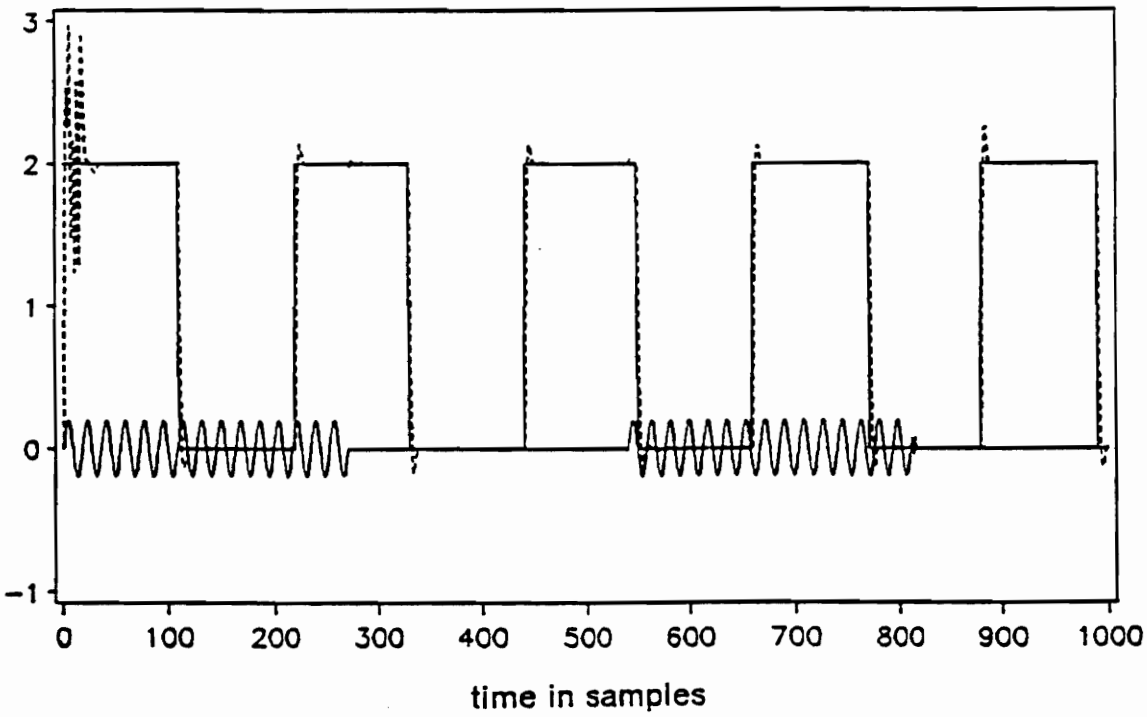

Figure 2. **Tracking performance and disturbance regulation:** (__) **reference and disturbance signals and** (—) **system output.**

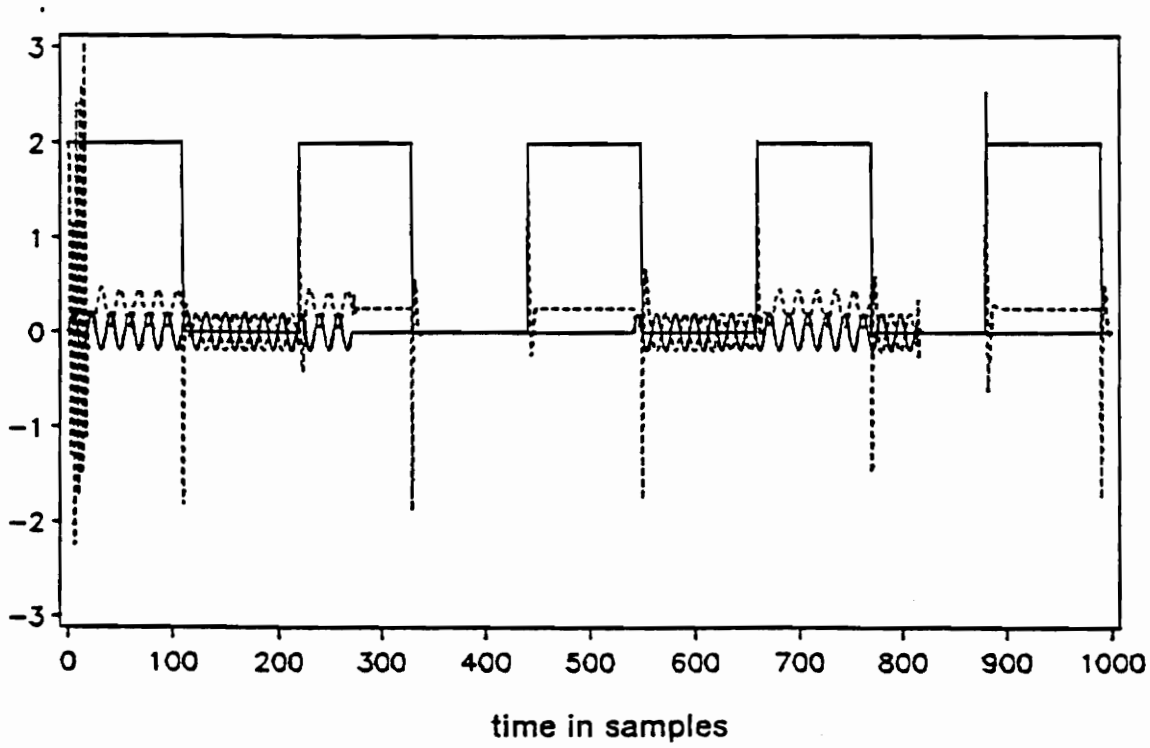

Figure 3. **Control input:** (__) reference and disturbance signals and (—) control input.

CHAPTER 3

DETERMINISTIC QUENCHING ALGORITHMS

3.1 Introduction

The deterministic quenching algorithms are for single-degree-of-freedom systems with quadratic and cubic nonlinearities governed by the equation

$$\ddot{x} + 2\mu\dot{x} + \omega_0^2 x + \alpha_2 x^2 + \alpha_3 x^3 + d_1 x = d_2 + d_3 \tag{3.1a}$$

$$d_i = f_i \cos(\Omega_i t + \tau_i), \quad i = 1,2,3 \tag{3.1b}$$

where ω_0, μ, α_2 and α_3 are unknown constant system parameters. One of the d_i will represent a sinusoidal disturbance with unknown amplitude, frequency and phase while one of the remaining d_i will act as the control signal. The disturbance sinusoid can enter the system in a parametric or external fashion.

In either case, the proper choice of the control sinusoid can greatly reduce the steady-state system response. For a comprehensive review of the response of single- and multi-degree-of-freedom systems to parametric and external excitations, we refer the reader to the textbook of Nayfeh and Mook [16].

In the next chapter the disturbance and unknown parameters will be incorporated into the system model and then the augmented system estimated. From the estimates the quenching signal will be generated and become an input to the process. The method is comparable to the internal model principle which for linear systems reduces to direct disturbance cancellation. In light of this the deterministic quenching algorithm will be compared to direct disturbance cancellation and the possible advantages of quenching highlighted.

Since the system parameters are unknown, the actual system may have a variety of different possible characteristics determined by its equilibrium points. The equilibrium points of undamped free oscillations of the system governed by Eq. (3.1) are given by $\omega_0^2 x + \alpha_2 x^2 + \alpha_3 x^3 = 0$. The system could have any of the following set of equilibrium points: one stable, one stable and one unstable, two stable and one unstable, or one stable and two unstable. Although the quenching algorithm is general, all examples will be given for the same system for comparison purposes. The actual system will have equilibrium points at $(x, \dot{x}) = (0,0)$,($-0.5,0$) and ($-1.0,0$) corresponding to the system parameters $\omega_0 = 1$, $\alpha_2 = 3$, and $\alpha_3 = 2$. The points (0,0) and (-1.0,0) are

centers while the point (-0.5,0) is a saddle point. For different excitations or initial conditions, the steady-state response of the system may be a small oscillation around either center or a large oscillation encircling all three equilibrium points. Figure 4 shows the phase plane with the three possible solutions of the undamped and unforced system.

Quenching is a phenomenon in nonlinear systems that results from the interaction of two different resonant excitations. It is the interaction of the two sinusoids that causes the quenching of the system response defined in Eqs. (3.1); therefore in the deterministic case it is irrelevant which sinusoid is called the disturbance and which is considered the control. In the next two sections, we assume that all parameters in Eqs. (3.1) are known and present the quenching requirements for the two cases considered in this thesis.

3.2 Parametric and Subharmonic Resonant Case

Using the perturbation method of multiple scales [17,18], Nayfeh [12] analyzed the interaction of principal parametric resonances with subharmonic resonances of order one-half in systems governed by Eq. (3.1). To obtain uniform solutions for this case, we rewrite Eq. (3.1) as

$$\ddot{x} + 2\mu\dot{x} + \omega_0^2 x + \alpha_2 x^2 + \alpha_3 x^3 + x f_1 \cos(\Omega_1 t + \tau) = f_2 \cos(\Omega_2 t) \qquad (3.2)$$

where μ, f_1, and f_2 are order (ε^2); $\alpha_2, \alpha_3, \omega_0, \Omega_1, \Omega_2$ are order (1); and ε is a small dimensionless parameter that indicates the relative size of the parameters. Both Ω_1 and Ω_2 are approximately $2\omega_0$ and τ is the relative phase between the two sinusoids. Under these assumptions, the perturbation analysis yields a second-order approximate solution given by

$$x = \varepsilon a \cos\left(\frac{1}{2}\Omega_2 t + \gamma_1\right) + \varepsilon^2\left[\frac{\alpha_2 a^2}{6\omega_0^2}\cos(\Omega_2 t + 2\gamma_1) - \frac{\alpha_2 a^2}{2\omega_0^2} - \frac{f_2}{\Omega_2^2 - \omega_0^2}\cos(\Omega_2 t)\right] + 0(\varepsilon^3) \tag{3.3}$$

where in general a and γ_1 (amplitude and phase modulation) satisfy a pair of highly nonlinear differential equations for which different solutions may exist for different initial conditions of the system states. Optimal quenching of the system response will occur if

$$\Omega_1 = \Omega_2, \quad \tau = 0, \quad f_1 = \frac{2\alpha_2 f_2}{(\Omega_2^2 - \omega_0^2)} \pm 4\omega_o\mu \tag{3.4}$$

If the quenching requirements are satisfied, $a = 0$ and Eq. (3.3) becomes

$$x = -\frac{\varepsilon^2 f_2}{\Omega_2^2 - \omega_0^2}\cos(\Omega_2 t) + 0(\varepsilon^3) \tag{3.5}$$

In Eqs. (3.3) and (3.5), ε indicates the relative size of the terms and should be set equal to unity when computations are performed. The quenched response is essentially the steady-state linear response of the system to the

subharmonic excitation. The quenched response is not dependent on initial conditions and will be the same for all initial conditions for which quenching occurs.

The relationship between f_1 and f_2 in Eq. (3.4) is good only if the assumption that both f_1 and f_2 are order (ε^2) is not violated. If the subharmonic excitation is considered the disturbance with the numerical values $\Omega_2 = 2.0$ and $f_2 = 0.06$, then the quenching algorithm requires that $\Omega_1 = 2.0, f_1 = 0.12$ and $\tau = 0$. Figure 5 shows the quenched system response in comparison with the system response if only the disturbance was present when $\mu = 0.01$. The quenched response is a pure sinewave with an amplitude of 0.02 which agrees well with Eq. (3.5). Figures 6, 7 and 8 show the maximum deviation from zero of the system response for both quenching and disturbance cancellation when the control sinusoid parameters are varied. Figures showing the maximum deviation of the system response versus a control sinusoid parameter were obtained by integrating the governing equations to steady state for a wide range of control parameter values. In the figures showing the influence of variations in the amplitude and frequency of the control signal, the response magnitude is plotted versus the ratio of the actual parameter value to the optimal parameter value. Maximum quenching can still occur for relatively large deviations from the optimal values of the phase and amplitude of the control sinusoid. Figure 8 highlights the fact that quenching and disturbance cancellation are very dependent on the use of the correct control frequency. The quenching algorithm is preferable to direct cancellation if the control

signal cannot enter the process in the same manner as the disturbance. In the present example, an external disturbance can be quenched using a control signal that enters the process in a parametric fashion.

3.3 Primary and Superharmonic Resonant Case

Nayfeh [10] considered the quenching of a primary resonance by a superharmonic resonance of order two in systems governed by Eq. (3.1). To perform the perturbation analysis, we rewrite Eq. (3.1) as

$$\ddot{x} + 2\mu\dot{x} + \omega_0^2 x + \alpha_2 x^2 + \alpha_3 x^3 = f_1 \cos(\Omega_1 t + \tau) + f_2 \cos(\Omega_2 t) \qquad (3.6)$$

where f_1 is order (ε^2), μ and f_2 are order (ε), and $\alpha_2, \alpha_3, \omega_0, \Omega_1$, and Ω_2 are order (1). For this case $\Omega_1 \approx \omega_0$, $2\Omega_2 \approx \omega_0$ and τ is again the relative phase between the two sinusoids. The perturbation analysis results in a second-order approximate solution of the form

$$
\begin{aligned}
x = {} & \varepsilon a \cos(\Omega_1 t - \gamma_1 + \tau_1) + \frac{4\varepsilon f_2}{4\omega_0^2 - \Omega_1^2} \cos\left(\frac{1}{2}\Omega_1 t + \tau\right) \\
& + \varepsilon^2 \left[\frac{16\mu\Omega_1 f_2}{(4\omega_0^2 - \Omega_1^2)^2} \sin\left(\frac{1}{2}\Omega_1 t + \tau\right) + \frac{\alpha_2 a^2}{6\omega_0^2} \cos(2\Omega_1 t - 2\gamma_1 + 2\tau_1) \right. \\
& + \frac{16\alpha_2 f_2 a}{\Omega_1(\Omega_1 + 4\omega_0)(4\omega_0^2 - \Omega_1^2)} \cos\left(\frac{3}{2}\Omega_1 t - \gamma_1 + \tau + \tau_1\right) \\
& + \frac{16\alpha_2 f_2 a}{\Omega_1(\Omega_1 + 4\omega_0)(4\omega_0^2 - \Omega_1^2)} \cos\left(\frac{1}{2}\Omega_1 t - \gamma_1 + \tau - \tau_1\right) \\
& \left. - \frac{\alpha_2 a^2}{2\omega_0^2} - \frac{8\alpha_2 f_2^2}{\omega_0^2(4\omega_0^2 - \Omega_1^2)^2} \right] + 0(\varepsilon^3),
\end{aligned}
\tag{3.7}
$$

The variables a and γ_1 satisfy a pair of highly nonlinear differential equations whose solution vary with different initial conditions. The requirements for optimal quenching of the system response are

$$
\Omega_1 = 2\Omega_2, \quad \tau = \tau_2 - \tau_1, \quad f_1 = \left(|\Gamma_2| / |\Gamma_1|\right) f_2^2 \tag{3.8}
$$

where

$$
\Gamma_1 = |\Gamma_1| e^{i\tau_1} = 1 - \frac{(\sigma - i\mu)}{2\omega_0} \tag{3.9}
$$

$$
\Gamma_2 = |\Gamma_2| e^{i\tau_2} = \left[1 - \frac{(\sigma - i\mu)}{2\omega_0} + \frac{4i\mu\Omega_2}{\Omega_2^2 - \omega_0^2} \right] \frac{\alpha_2}{2(\Omega_2^2 + \omega_0^2)^2} \tag{3.10}
$$

$$
\sigma = \Omega_1 - \omega_0 \tag{3.11}
$$

Satisfying the quenching requirements results in a = 0 and Eq. (3.7) being reduced to

$$x = \frac{4\varepsilon f_2}{4\omega_0^2 - \Omega_1^2}\left(\cos\frac{1}{2}\Omega_1 t + \tau\right) + \varepsilon^2\left[\frac{16\mu\Omega_1 f_2}{(4\omega_0^2 - \Omega_1^2)^2}\sin\left(\frac{1}{2}\Omega_1 t + \tau\right) - \frac{8\alpha_2 f_2^2}{\omega_0^2(4\omega_0^2 - \Omega_1^2)^2}\right] + 0(\varepsilon^3), \tag{3.12}$$

The quenched response is again basically the steady-state linear response of the system to the superharmonic excitation, but in this case there is also a small constant offset present.

If we let the disturbance be the superharmonic excitation with the numerical values $f_2 = 0.08$ and $\Omega_2 = 0.525$, then the parameters of the control sinusoid are $f_1 = 0.0183$, $\Omega_2 = 1.05$ and $\tau = -0.01486$. Figure 9 shows the system response to the disturbance (no control) along with the quenched response. The disturbance response is an example of the large oscillation in Figure 4. Figures 10, 11, and 12 show the maximum deviations from zero of the steady-state response of the system for variations of the control sinusoid parameters. Simulations indicate that when quenching a large oscillation the response may go from a quenched response to an unquenched one and back to a quenched response for very small changes in any of the control sinusoid parameters. Except for a slight disadvantage in frequency, direct disturbance cancellation can reduce the system response considerably for a much larger range of values near the optimal amplitude and phase. The advantage of

quenching lies in the reduced control effort required. The perturbation analysis shows that the amplitude of the primary excitation needed for quenching the response is an order of magnitude smaller than the amplitude of the superharmonic excitation. In the previous example the disturbance is more than four times larger than the control and can be greater for a smaller value of α_2.

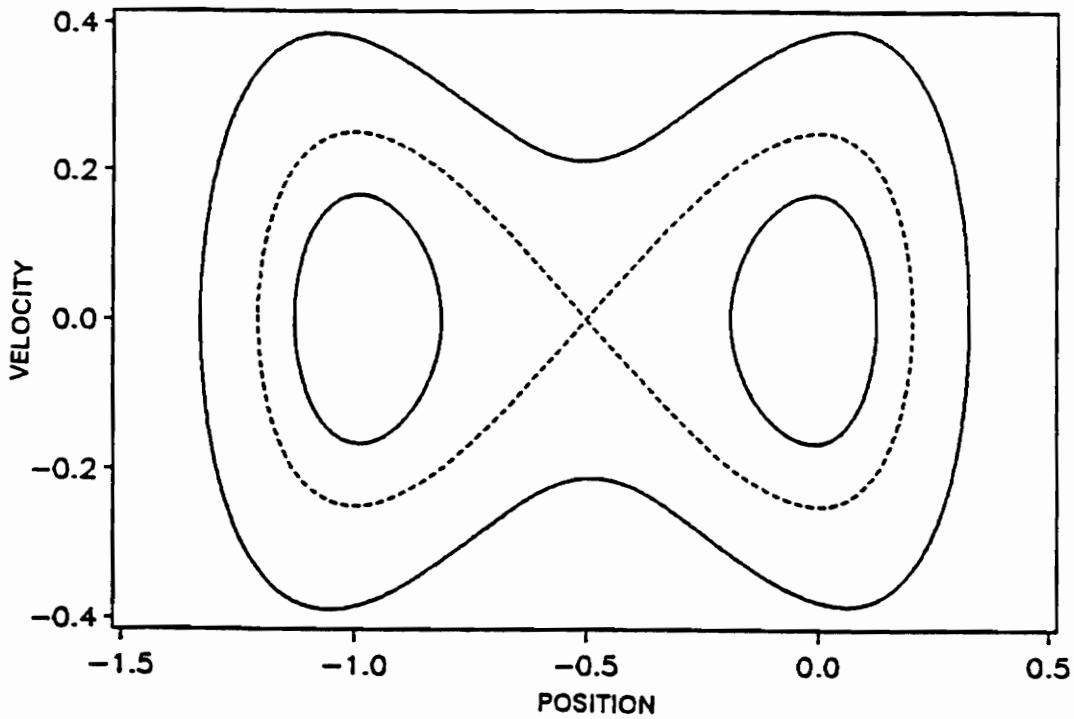

Figure 4. Phase plane for the undamped and unforced system corresponding to the parameters $\omega_0 = 1$, $\alpha_2 = 3$, $\alpha_3 = 2$, $\mu = 0.01$: (__) possible system solutions and (—) separatrices.

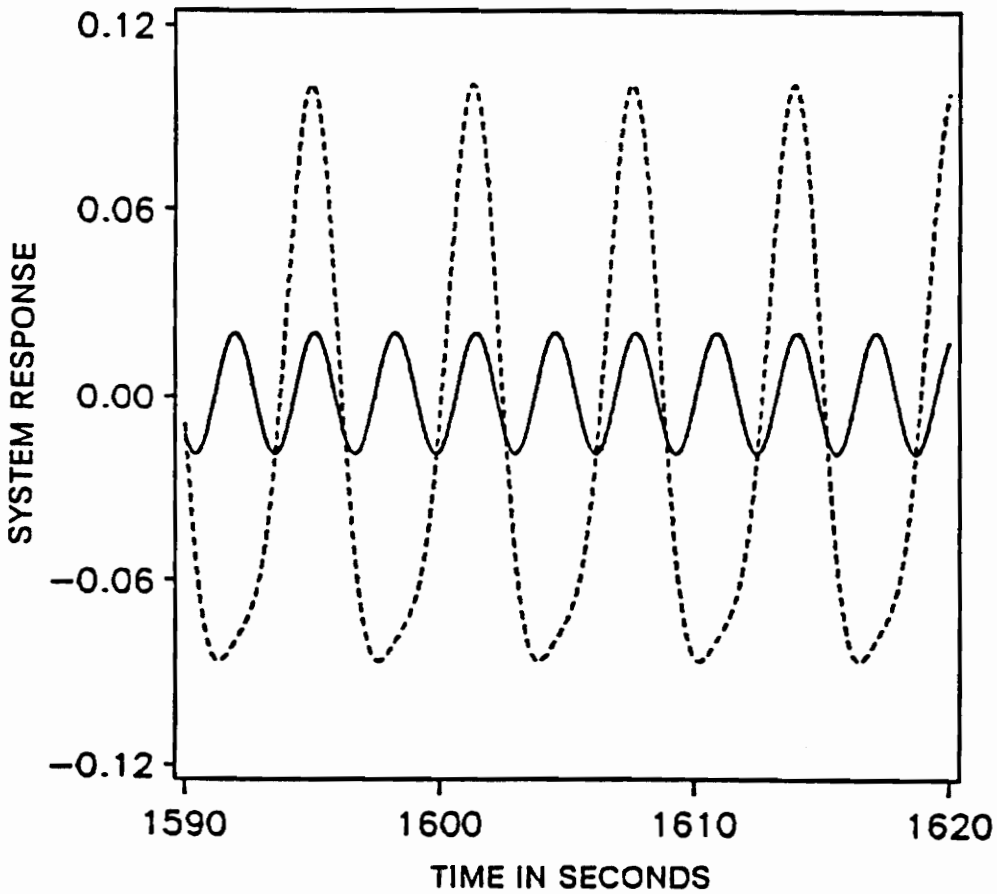

Figure 5. Disturbance and quenched responses for the parametric/subharmonic resonant case: (__) quenched response and (—) response to disturbance

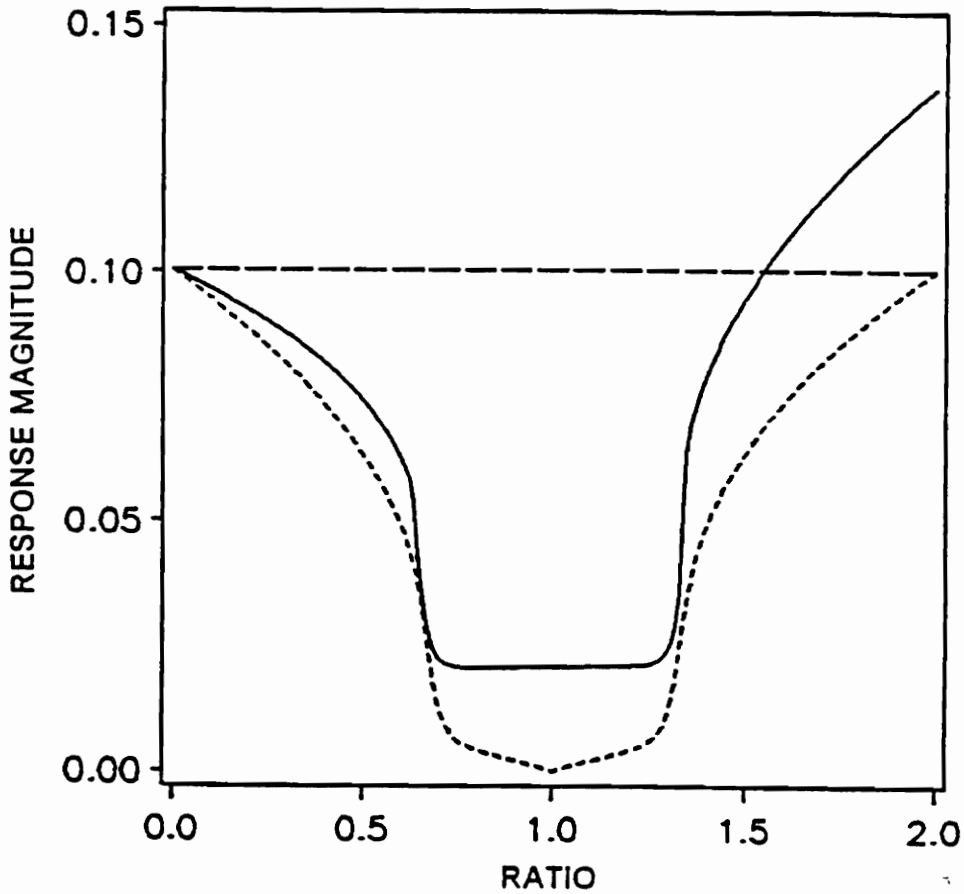

Figure 6. Influence of variations in control amplitude on the response magnitude for the parametric/subharmonic resonant case: (__) quenched response, (---) disturbance cancellation, and (__ __ __) no control.

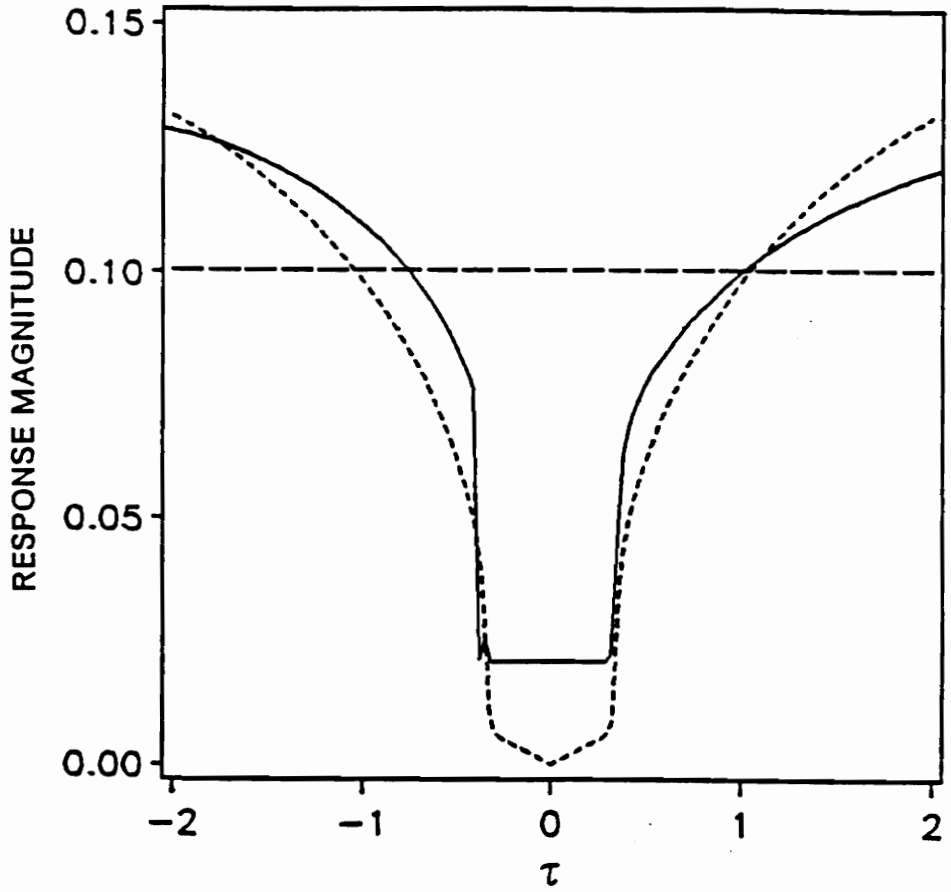

Figure 7. Influence of variations in control phase on the response magnitude for the parametric/subharmonic resonant case: (__) quenched response, (—) disturbance cancellation, and (_ _ _) no control.

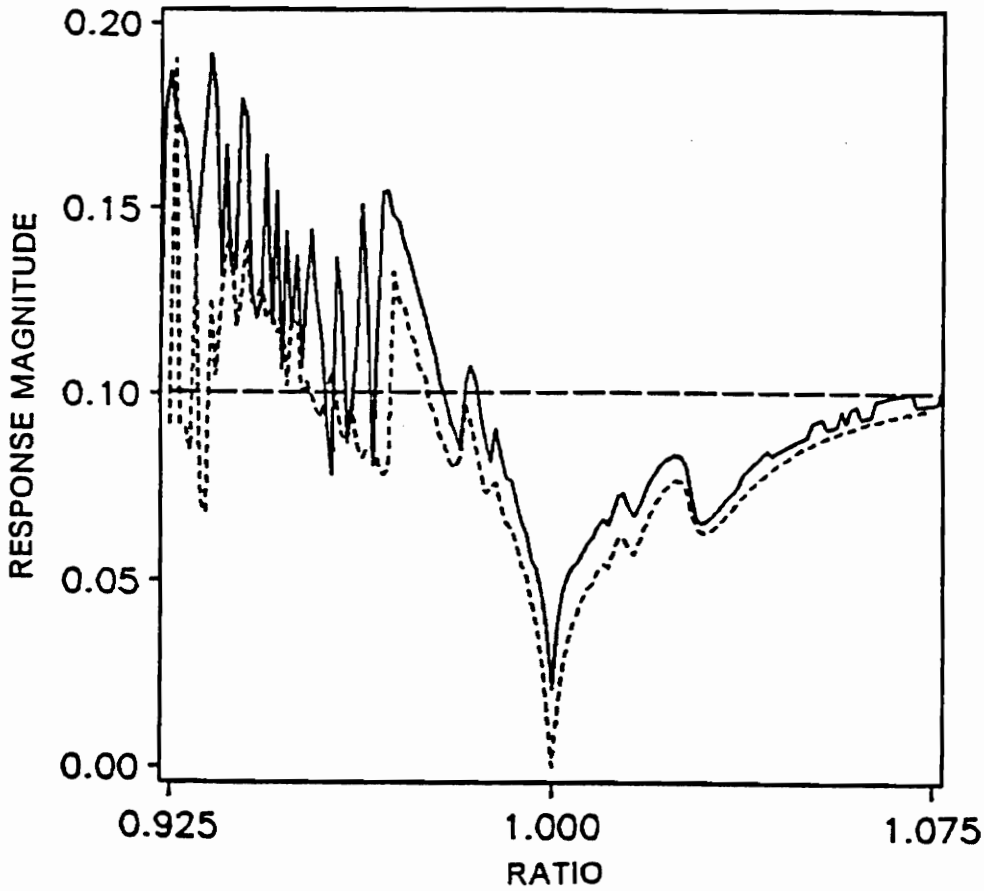

Figure 8. Influence of variations in control frequency on the response magnitude for the parametric/subharmonic resonant case: (__) quenched response, (—) disturbance cancellation, and (__ __ __) no control.

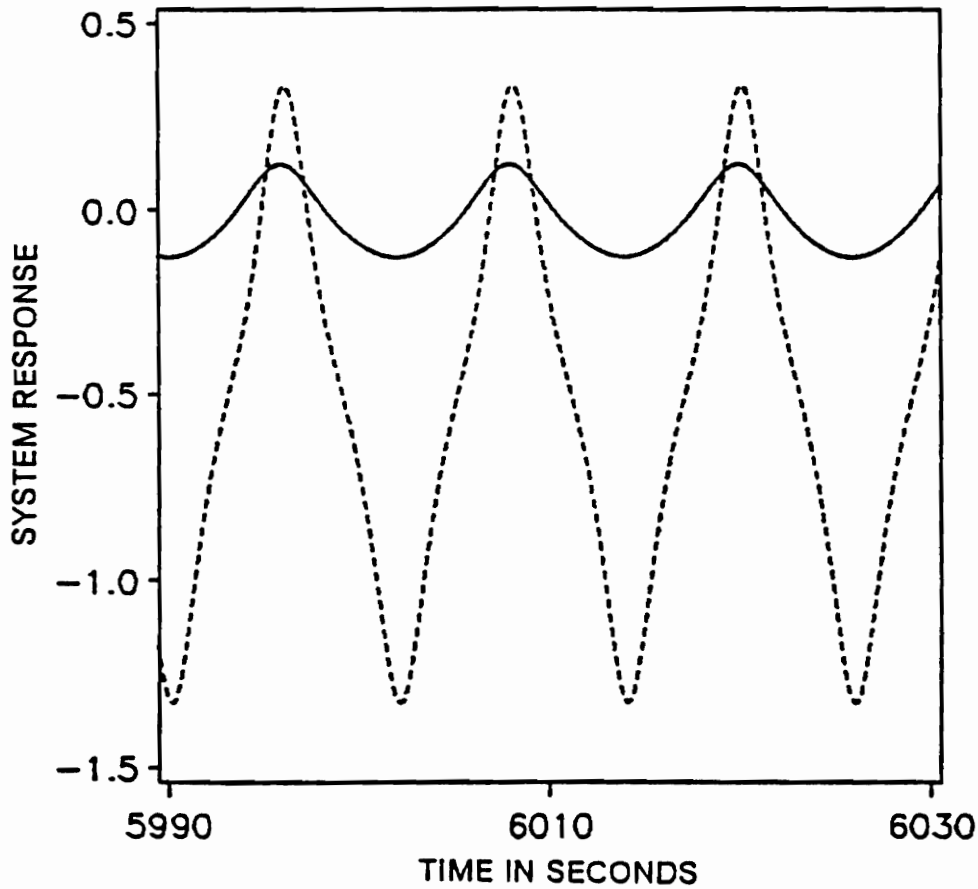

Figure 9. Disturbance and quenched responses for the primary/superharmonic resonant case: (__) quenched response and (---) response to disturbance

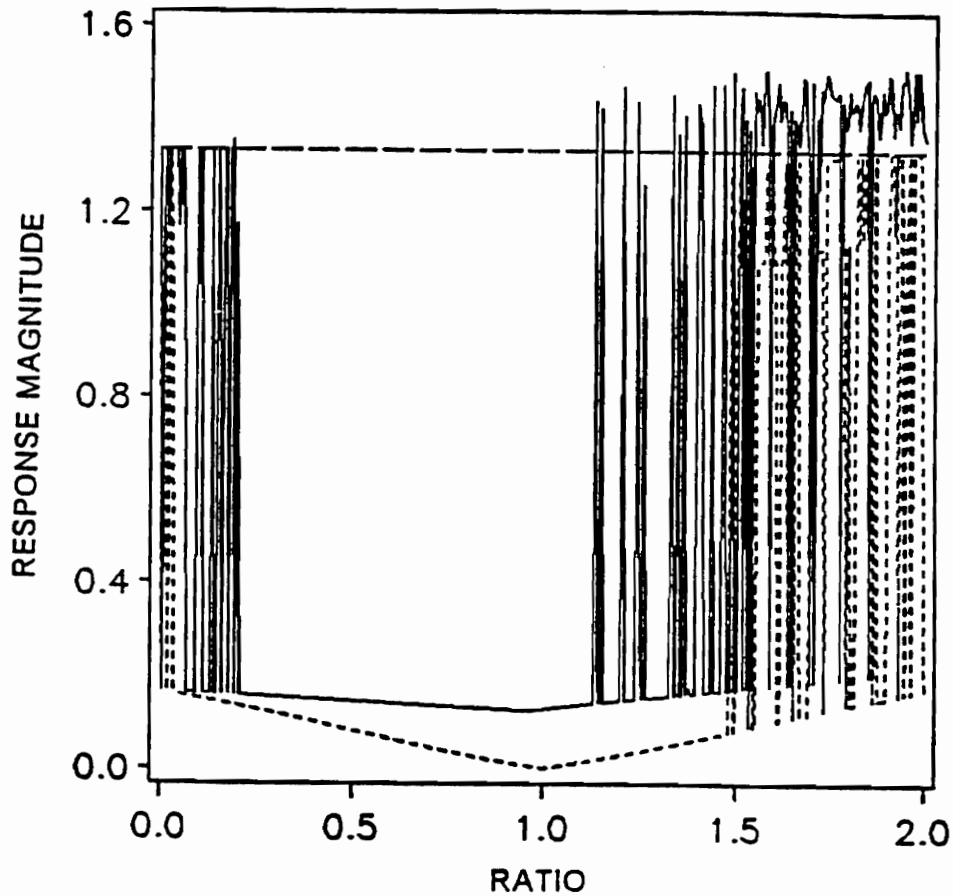

Figure 10. Influence of variations in control amplitude on the response magnitude for the primary/superharmonic resonant case: (__) quenched response, (---) disturbance cancellation, and (_ _ _ _) no control.

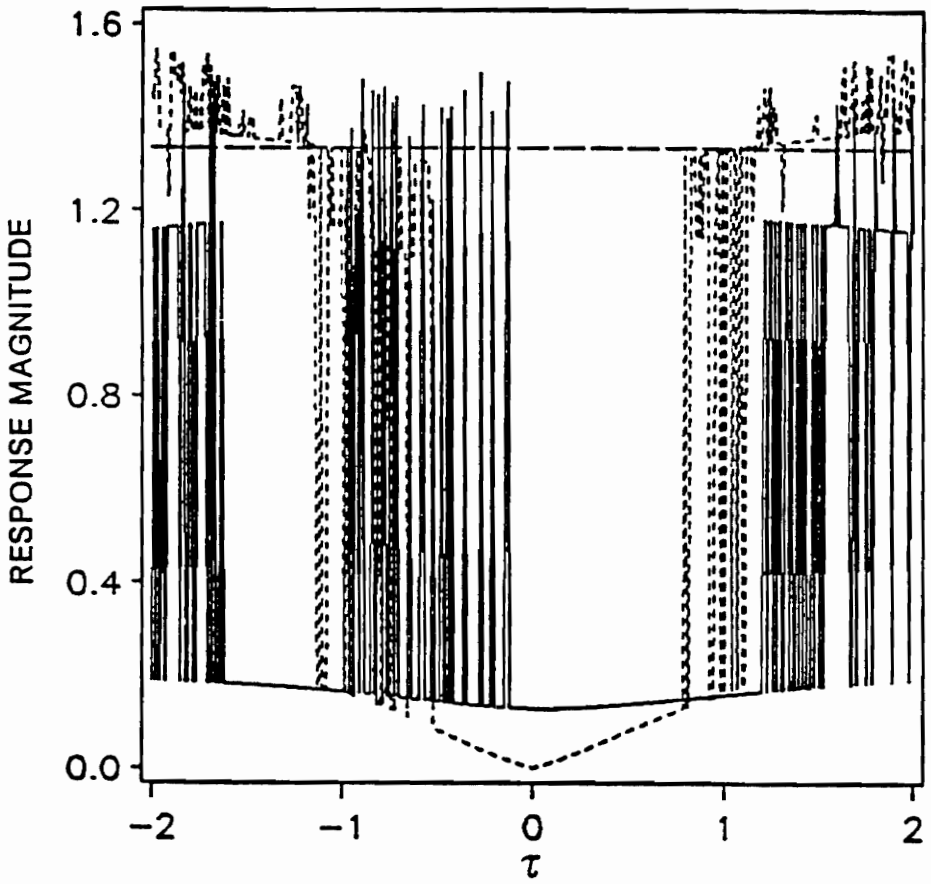

Figure 11. Influence of variations in control phase on the response magnitude for the primary/superharmonic resonant case: (__) quenched response, (—) disturbance cancellation, and (__ __ __) no control.

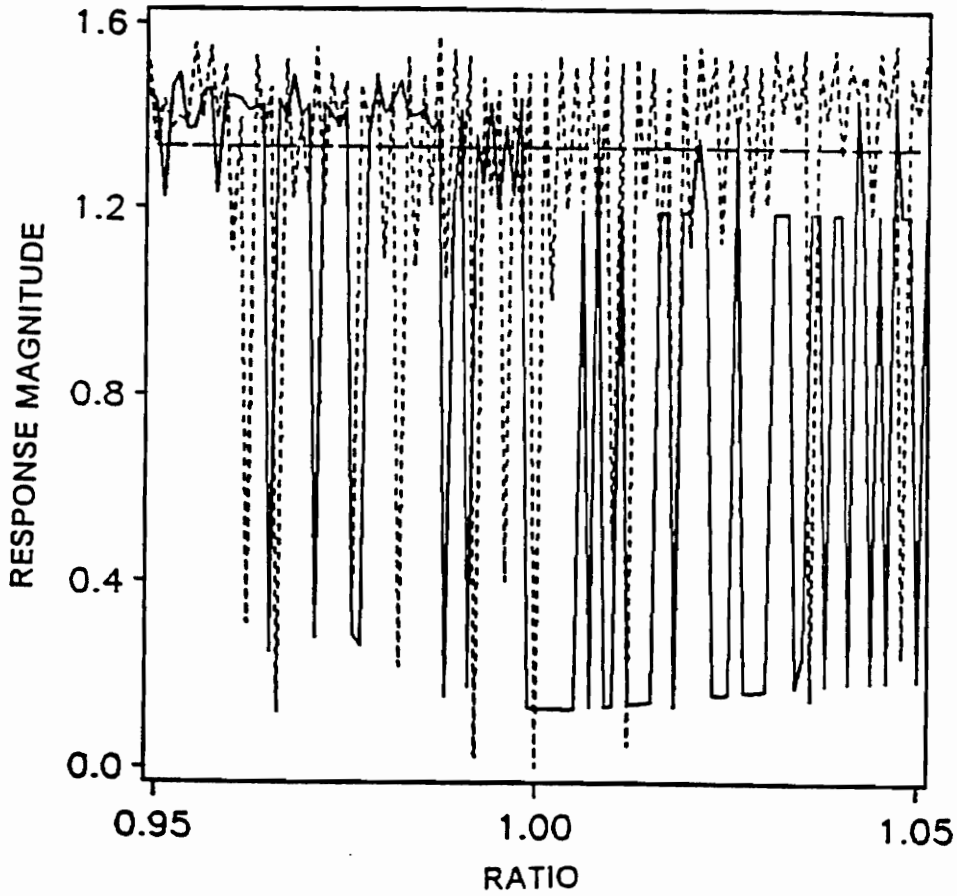

Figure 12. Influence of variations in control frequency on the response magnitude for the primary/superharmonic resonant case: (__) quenched response, (---) disturbance cancellation, and (__ __ __) no control.

CHAPTER 4

ADAPTIVE QUENCHING ALGORITHMS

4.1 The Modified EKF Equations

The previous deterministic quenching algorithms are implemented adaptively using an indirect method. A modified EKF is used to estimate the disturbance and the unknown parameters. The parameter estimates are used to update the control sinusoid every n seconds. If at time T_n there is no disturbance present, the control is set equal to zero. Equation (3.1) can be written as $\dot{x}_s = f(x_s, x_\theta, u)$ where x_s includes the two system states and the disturbance sinusoid, x_θ is a vector composed of all the unknown constant system and disturbance parameters, and u is the control sinusoid. If the appropriate noise processes are added to the system, the standard EKF [19] along with its modifications are given by the following equations:

The system and measurement models are

$$x_T = \begin{bmatrix} x_s \\ x_\theta \end{bmatrix} \tag{4.1}$$

$$\dot{x}_s = f[x_s(t), x_\theta, u] + w(t); \quad w(t) \sim N[0, Q(t)] \tag{4.2}$$

$$\dot{x}_\theta = 0 \tag{4.3}$$

$$Z_k = h_k[x_T(t_k)] + v_k; \quad k = 1, 2, 3, \ldots; \quad v_k \sim N(0, R_k) \tag{4.4}$$

The propagation equations are

$$\dot{\hat{x}}_s(t) = f[\hat{x}_s(t), \hat{x}_\theta(t), u] \tag{4.5}$$

$$\dot{P}(t) = F[\hat{x}_T(t)]P(t) + P(t)F^T[\hat{x}_T(t)] \tag{4.6}$$

The gain matrix is

$$K_k = P(t_k -)H_K^T(\hat{x}_T(t_k -))\left[H_k(\hat{x}_T(t_k -))P(t_k -)H_k^T(\hat{x}_T(t_k -)) + R_k\right]^{-1} \tag{4.7}$$

The update equations are

$$\hat{x}'_T(t_k +) = \hat{x}_T(t_k -) + K_k\left[Z_k - h_k(\hat{x}(t_k -))\right] \tag{4.8}$$

$$P(t_k +) = \left[I + K_k H_k(\hat{x}_T(t_k -))\right]P(t_k -) \tag{4.9}$$

where

$$F(\hat{x}_T(t)) = \frac{\partial f(x_T(t), u)}{\partial x_T(t)} \Big|_{x_T(t) = \hat{x}_T(t)} \tag{4.10}$$

$$H_k(\hat{x}_T(t_k -)) = \frac{\partial h_k(x_T(t_k))}{\partial x_T(t_k)} \Big|_{x_t(t_k) = \hat{x}_T(t_k -)} \tag{4.11}$$

$$x_T(0) \sim N(\hat{x}_0, P_0) \text{ and } E\left[w(t) v_k^T \right] = 0 \text{ for all k and t}$$

At $t_k = mT_n$, $m = 1,2,3,...$, we let the error covariance matrix be partitioned as

$$P = \begin{bmatrix} P_s & P_{s\theta} \\ P_{\theta s} & P_\theta \end{bmatrix}$$

where P_s and P_θ are square matrices with dimensions equal to the dimension of their associated state vector. Now we define the following quantities:

P_{diag} = P with all but the diagonal elements set to zero,

D_θ = vector composed of the diagonal elements of P_θ,

$N_\theta = \|D_\theta\|_2$, and

$E_{\theta, m} = (N_{\theta, m-1} - N_{\theta, m})/N_{\theta, m-1}$

Based on the above information, the modified update equations at $t_k = mT_n$, $m = 1,2,3,...$, become

$$P = P_{\text{diag}} \tag{4.12}$$

$$\hat{x}_s = \hat{x}'_s \tag{4.13}$$

$$\hat{x}_\theta = \begin{cases} \hat{x}'_\theta & \text{if } E_{\theta,m} \geq \delta \\ \hat{x}'_\theta \text{ at } t_k = (m-1)T_n & \text{if } E_{\theta,m} < \delta \end{cases} \tag{4.14}$$

where δ is a design parameter.

4.2 Performance Analysis

It is well documented in the literature [19] that the estimates obtained from a standard EKF can be biased and have a tendency to drift after the filter reaches steady state. These problems are magnified in the present case because the system has a low level of excitation. The biased estimates may cause the algorithm to use a control sinusoid that will not be able to quench the response as evidenced by Figures 6-8 and 10-12. Figures 13, 14, and 15 show that resetting the phase of the control signal every T_n seconds significantly reduces the need for an extremely accurate estimate of the disturbance frequency.

The steady-state estimate bias can be reduced by resetting the error covariance every T_n seconds and allowing the filter to reconverge starting with

a better set of initial estimates. A common practice in linear systems is to reset the error covariance to a constant diagonal matrix, say $P = k_0 I$. If the constant k_0 is large enough to ensure an adequate filter convergence rate at the beginning, the error covariance will be artificially large after several resettings when the estimates are near their actual values. In linear systems this causes no problem since the filter is guaranteed to converge to the system's proper values. For our system the artificially large error covariance can cause different and possibly worse steady-state errors in the estimates at every resetting. Even if the control sinusoid based on these biased estimates is within acceptable tolerances as demonstrated by Figures 6-8 and 10-12, the response may not be quenched as seen in Figure 16. The quenching algorithm requires that the control sinusoid be constant for an extended period of time to ensure quenching. This problem can be overcome if instead of $P = k_0 I$, the error covariance is reset to a diagonal matrix whose elements are the diagonal elements of the EKF's best estimate of the mean-square error of it's corresponding state estimate. Using Eq. (3.12) as the error covariance resetting rule allows the EKF to obtain better estimates with each successive resetting. The matrix P_{diag} will eventually reach steady state, indicating that the filter is unable to obtain better estimates with the current excitation.

Shortly after P_{diag} reaches steady state, the parameter estimates may start to drift slowly from their converged values. When P_{diag} reaches steady state, the condition $E_{\theta,m} < \delta$ will be true and Eq. (3.14) will keep the elements of $\hat{x}_\theta$ at their

converged values. Equation (3.13) allows the EKF to track the disturbance after the system has reached steady state.

As an example, we consider the parametric/subharmonic resonant case discussed previously. Equations (3.2) and (3.3) become the augmented system

$$\dot{x}_1 = x_2, \quad \dot{x}_2 = -x_6 x_2 - x_7 x_1 - x_8 x_1^2 - x_9 x_1^3 + x_3 - u x_1$$

$$\dot{x}_3 = x_4, \quad \dot{x}_4 = -x_5 x_3, \quad \dot{x}_5 = 0, \quad x_5 \equiv \Omega_2^2$$

$$\dot{x}_6 = 0, \quad x_6 \equiv 2\mu, \quad \dot{x}_7 = 0, \quad x_7 \equiv \omega_0^2$$

$$\dot{x}_8 = 0, \quad x_8 \equiv \alpha_2, \quad \dot{x}_9 = 0, \quad x_9 \equiv \alpha_3$$

For all adaptive quenching simulations a sampling rate of 20 Hz and position measurements are used. The noise statistics and initial conditions of the filter are given in Table 1. Figure 17 shows how P_{diag} reaches steady state ($E_{\theta,m} \rightarrow 0$) in a relatively short time. Figures 18 and 19 show the short and long term characteristics of the quantity $\mathcal{E} = \sum_{i=5}^{9} |x_i - \hat{x}_i| / x_i$. The estimated parameters reach steady-state values and then would drift as indicated by the dashed line in Fig. 19 if not for Eq. (3.14). Figures 17-19 show that the filter exhibits the best convergence properties for a resetting time of T_{20} = 20 seconds and this value is used in the remaining examples.

Figures 20 and 21 show how the algorithm performed for different initial conditions of position and velocity. For both the parametric/subharmonic and

the primary/superharmonic resonant cases the algorithm works well and consistently inside a quenching region defined by the separatrix encircling the origin. The perturbation analysis that leads to the deterministic quenching requirements assumed that the system response was a small oscillation about the origin. Even for initial conditions that seem to violate this assumption, the response may be quenched although it might be undesirable since it may linger for some time around the large solution in Figure 4 before converging to the quenched response. Since any steady-state response which is not quenched and centered at the origin is also undesirable, Figures 20 and 21 suggests the use of a hybrid control law where the quenching algorithm is used when the system states are inside the quenching region and a global control law is used outside this region.

4.3 Alternative Filters

Several other filters were tried and discarded in favor of the modified EKF used. To try to lessen the drift of the estimates, a method which overemphasizes the more recent observations was applied to the standard EKF. The method as described by Jazwinski [20] multiplies the measurement error covariance matrix by an exponential weighting factor less than unity before deriving the filter equations. The result is an increased covariance matrix and therefore an increased filter gain. The method is supposed to

prevent the filter from becoming too confident of its estimates based on past observations that it can not react adequately to new information caused either by a change in the system or in the excitation. The filter based on this method did not converge as well and experienced a faster drift than the filter used. The failure of the filter did highlight the fact that the information for identification is in the transient response and that the drift problem is caused by the low level of excitation.

Another filter that was tried was based on the Jump Matrix Technique [21,22]. By using fictitious samplers and clamps, the technique models the nonlinear system by a linear and nonlinear subsystem. The output of the nonlinear subsystem is updated at every sampling instance and then held constant until the next sample. The output of each nonlinearity is considered to be a state variable. The result is that the complete system is modeled as linear between samples with a nonlinear instantaneous 'jump' in the system states at the sampling instant. The filter equations are those of a Kalman filter with the exception of a nonlinear update equation for the state vector. The filter was simulated and compared against a standard EKF. The filter did not perform as well as the EKF and was discarded.

4.4 Analog-Computer Simulation

4.4.1 Setup and Verification

Equation (3.1) was simulated on an analog computer for the system parameters given in Chapter 3. The external sinusoidal disturbance was obtained using a Wavetek function generator. The adaptive algorithm was implemented using a 12 MHz personal computer with a 10 bit ADC and a 12 bit multiplying DAC to provide the interface between the analog and digital computers. Figures 22 and 23 show the limit cycles of the disturbance and quenched responses obtained from the analog-computer simulation. For both the parametric/subharmonic and primary/superharmonic resonant cases the algorithm performs adequately and obtains the desired quenched responses.

To provide enough time between samples to perform the required calculations, we reduced the sampling rate to 9 Hz. The reduced sampling rate combined with the implementation problems of non-Gaussian measurement noise, single precision arithmetic, and a nonideal real system caused the filter not to converge as well as in the digital-computer simulations. To partially compensate for the reduction in performance, we started the analog-computer simulations with a slightly better estimate of the system parameters.

4.4.2 Time and Magnitude Scaling

The analog computer was operated in the slow mode resulting in a natural frequency of approximately 0.157 Hz. To provide more time for the required calculations, we scaled the time to slow down the analog simulation by a factor of 10. The time scaling relation is given by

$$\tau = \beta t$$

where τ is the computer time, t is the real time, and β is the scale factor. In the present case $\beta = 10$ and the time scaling is achieved by multiplying each input of every integrator by $\frac{1}{\beta}$. The time scaling also requires that the frequency of each external excitation be multiplied by $\frac{1}{\beta}$. Running the analog computer in the slow mode and using the time scaling resulted in the simulations taking three to four hours to reach steady state. To obtain the most accurate results possible, one should magnitude scale the simulated equation to use the full range (-10v to 10v) of the analog computer. For the parametric/subharmonic resonant case, Eq. (3.2) was scaled using $\eta = 10x$. The scaled equation is given by

$$\ddot{\eta} + 2\mu\dot{\eta} + \omega_0^2\eta + 0.1\alpha_2\eta^2 + 0.01\alpha_3\eta^3 + ux = 10d$$

where d is the disturbance and u is the control sinusoid. The analog-patching diagram for the scaled equation is given in Figure 24. For the

primary/superharmonic resonant case, magnitude scaling was not possible and Eq. (3.6) was patched as shown in Figure 25.

4.4.3 Sources of Error

There were several sources of error in the analog simulations. The ADC board was found to have a small deadband centered at zero. The deadband was large enough to cause the EKF not to converge properly, therefore the sampled signal was offset by 6v, which was later removed in the software. A multiplying DAC is only able to attenuate an input voltage, therefore an offset voltage was necessary in order to produce the positive and negative values of a sinusoid. The amplitude of the sinewave produced by the multiplying DAC was larger than needed and later attenuated to the required value to reduce the effect of discretization. The sinewave also had a small dc offset which was partially compensated for by adjusting pot setting (3). The residual offset resulted in a shift in the natural frequency for the case of the parametric control and in a constant acceleration in the case of the external control. Another source of undesirable acceleration came from the multiplier circuits on the analog computer. The amplifier gains of the multiplier could not be sufficiently adjusted to obtain a zero output given a zero input. While this offset was only on the order of 10 mV, it was unmodeled and caused problems in identifying the system. The problem was especially acute for the

primary/superharmonic resonant case since the offset was roughly an eighth of the disturbance amplitude.

Table 1. Filter Parameters

$$\hat{x}_0 = [0 \;\; 0 \;\; 0 \;\; 0 \;\; 2.56 \;\; 0.04 \;\; 0.64 \;\; 0 \;\; 0]^T$$

$$P_s = 0.1I \quad P_{s\theta} = 0 \quad P_\theta = [100 \;\; 10 \;\; 100 \;\; 1000 \;\; 1000]$$

$$Q = 0.1I \quad R_K = 1x10^{-5} \quad \text{corresponding to } SNR_0 = 20$$

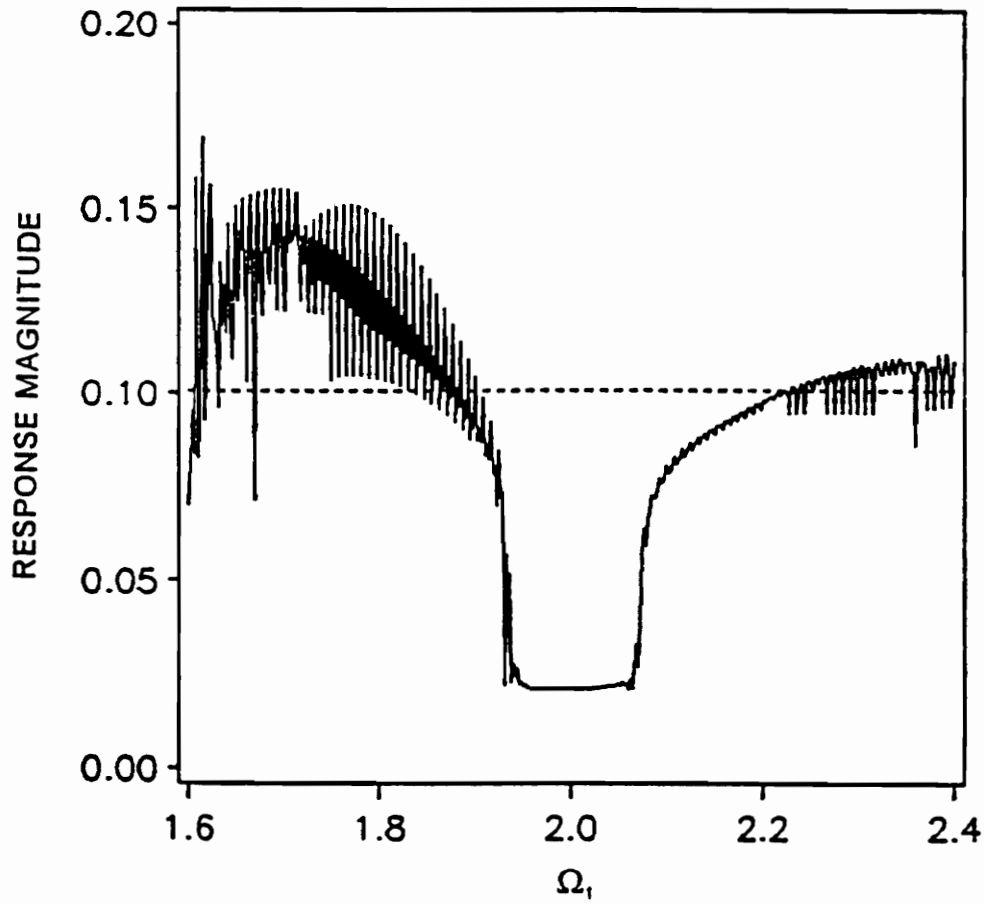

Figure 13. Influence of variations in control frequency on the response magnitude for the parametric/subharmonic case with T_{10}

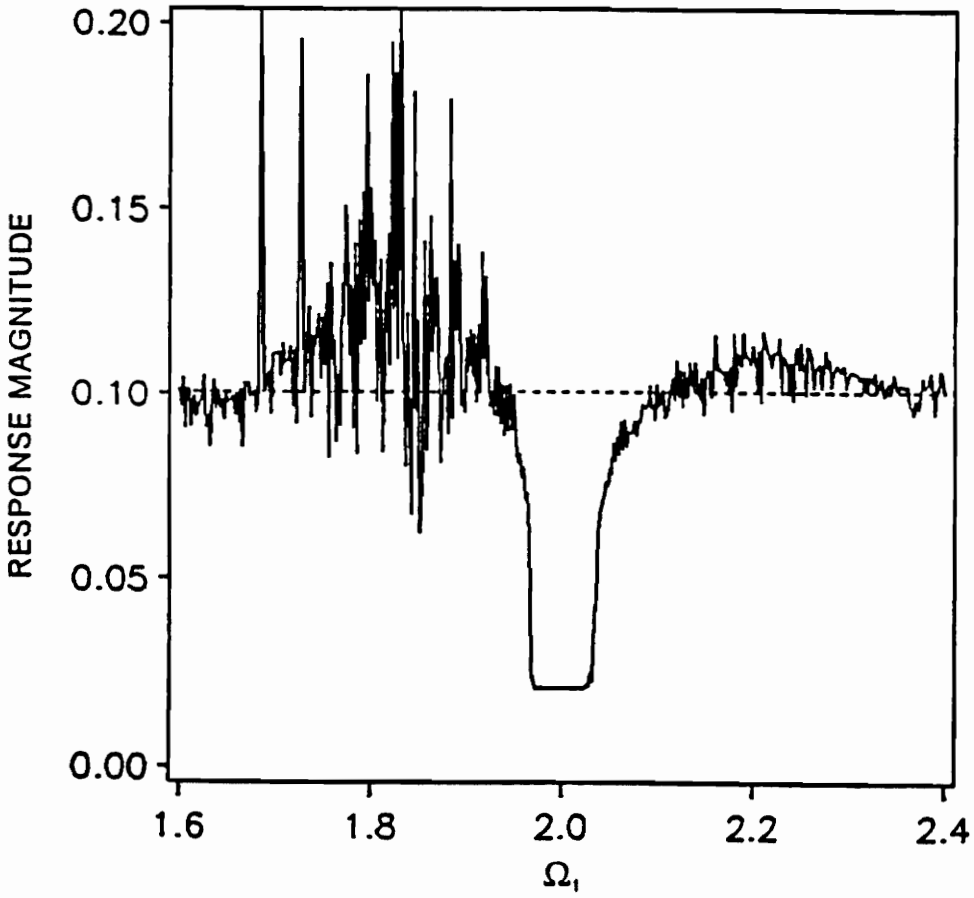

Figure 14. Influence of variations in control frequency on the response magnitude for the parametric/subharmonic case with T_{20}

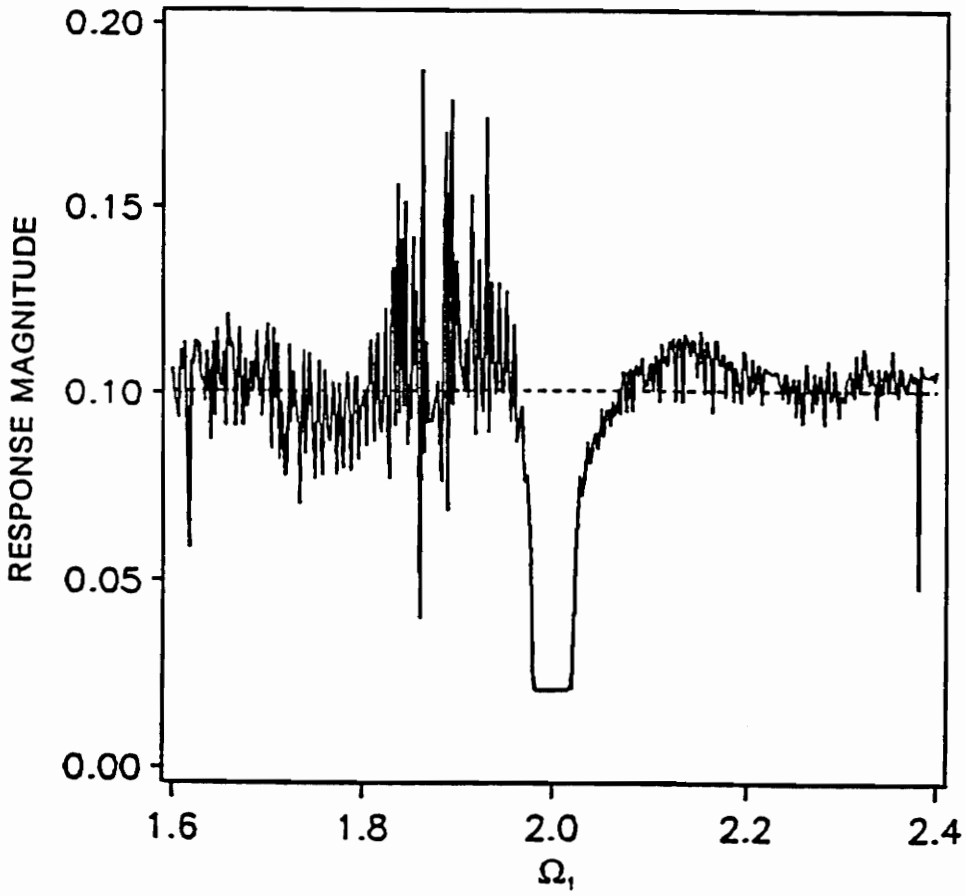

Figure 15. Influence of variations in control frequency on the response magnitude for the parametric/subharmonic case with T_{30}

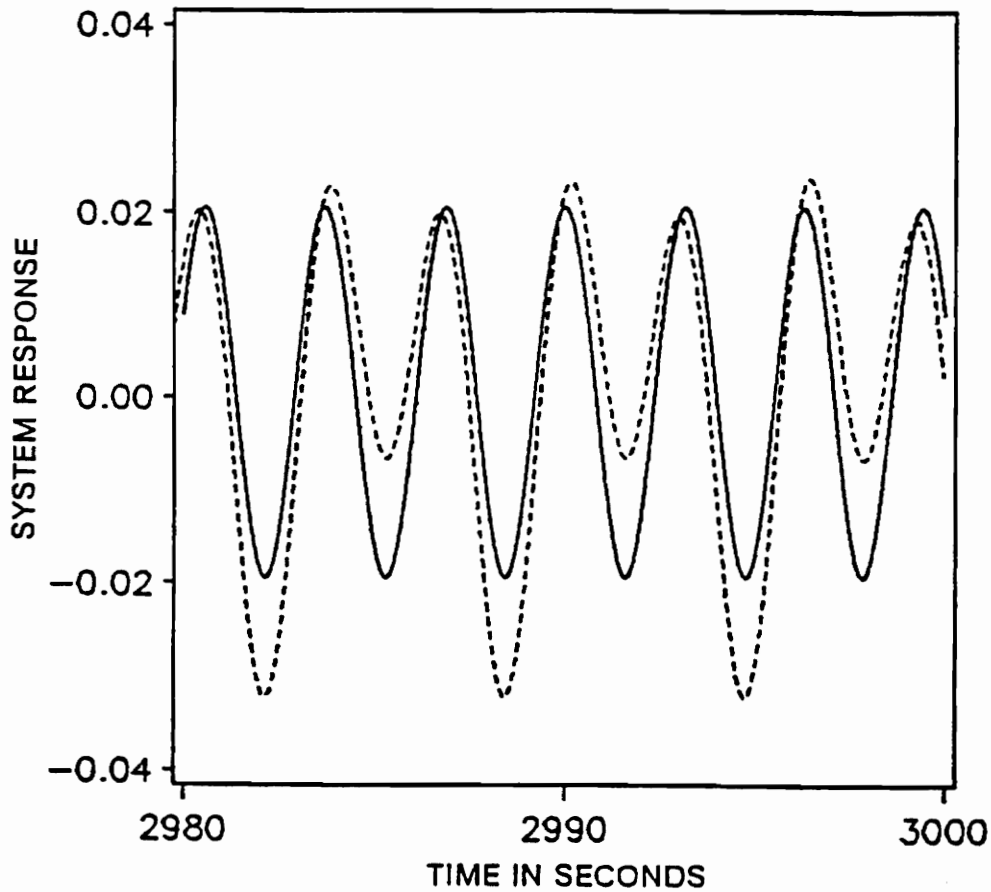

Figure 16. Effect of estimation errors: (__) properly quenched response and (- - -) improperly quenched response

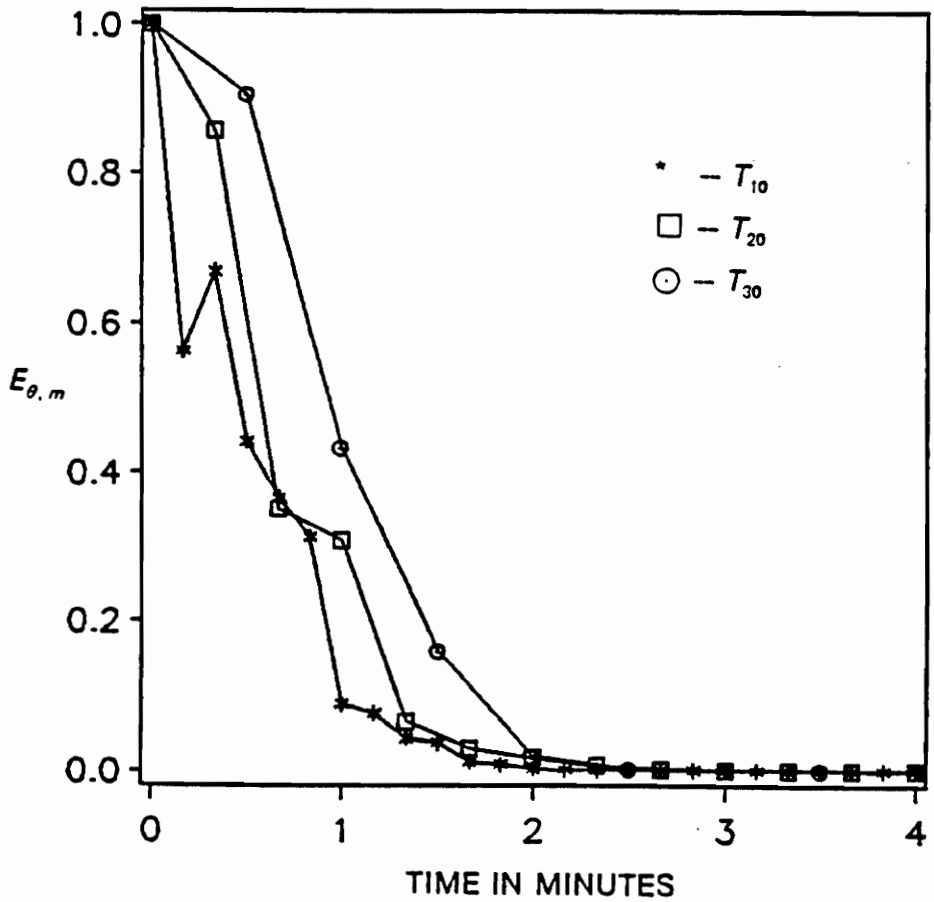

Figure 17. Variations of $E_{\theta,m}$

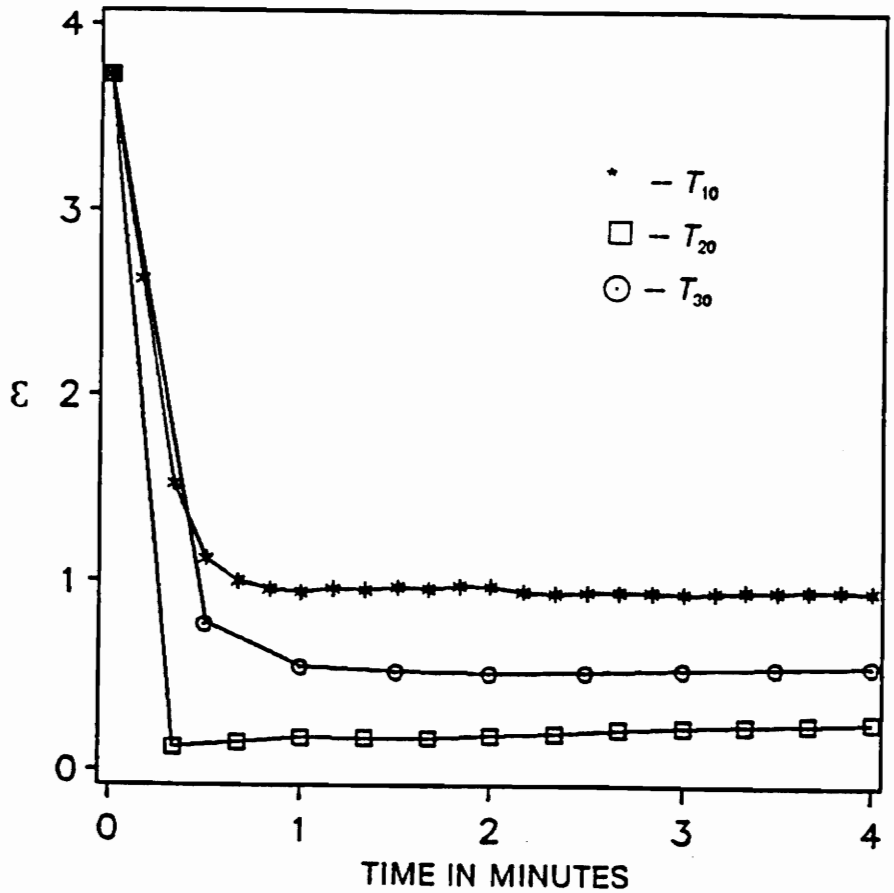

Figure 18. Short-term characteristics of ε

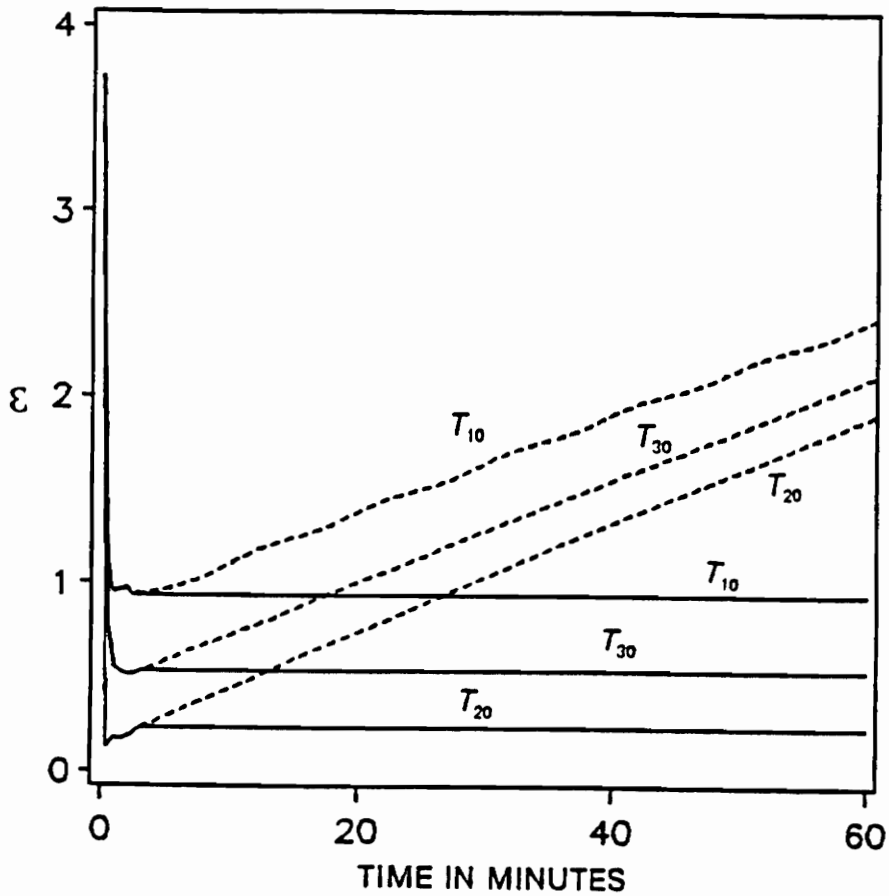

Figure 19. **Long-term characteristics of ε:** (__) EKF with modified update equations and (- - -) EKF with standard equations.

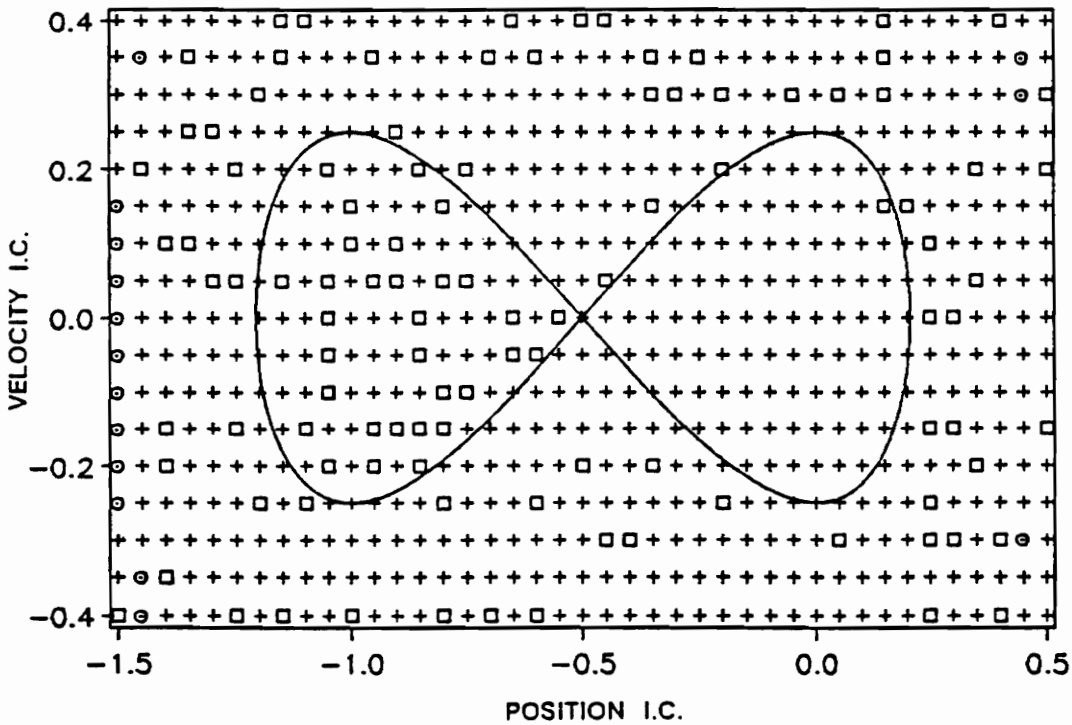

Figure 20. Convergence of the adaptive quenching algorithm for different initial conditions for the parametric/subharmonic resonant case: (+) quenched about the origin, (□) oscillation about x = - 1.0, and (⊙) large oscillation encircling all three equilibrium points and $\dot{x} = 0$.

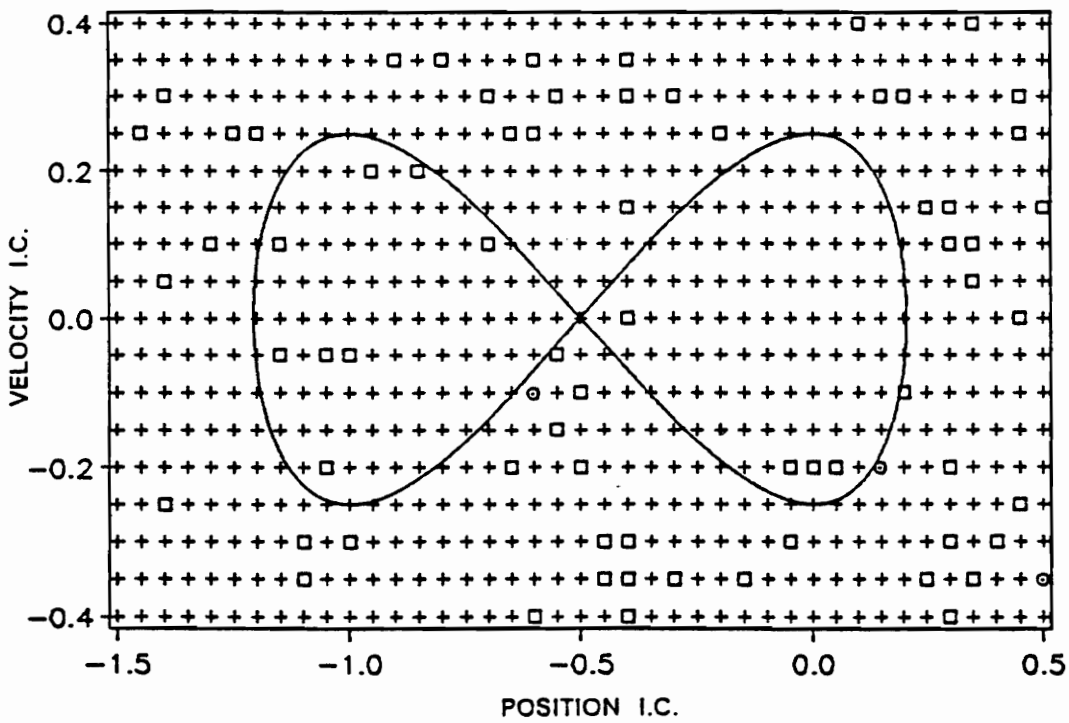

Figure 21. Convergence of the adaptive quenching algorithm for different initial conditions for the primary/superharmonic resonant case: (+) quenched about the origin, (□) oscillation about x = - 1.0, and (⊙) large oscillation encircling all three equilibrium points and $\dot{x} = 0$.

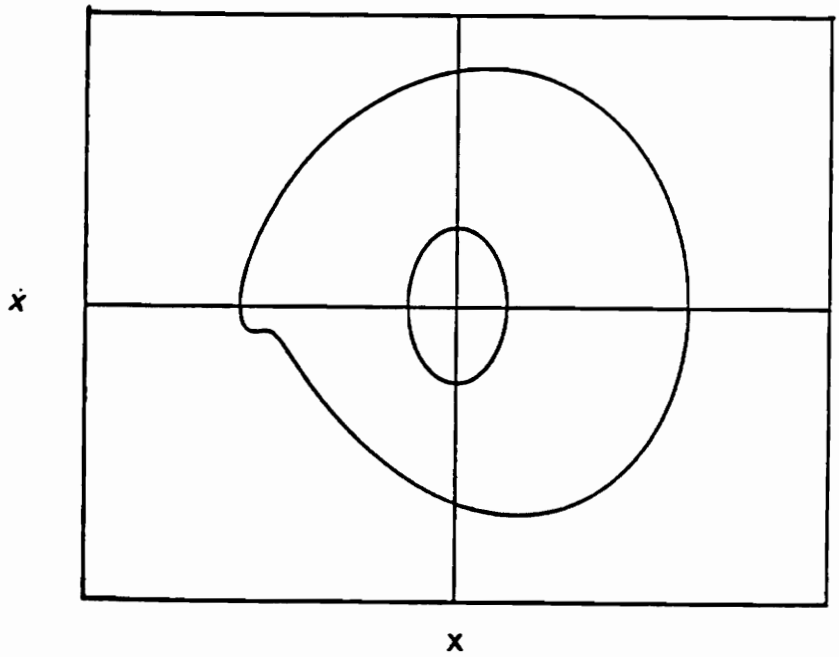

Figure 22. Limit cycles of the disturbance and quenched response from the analog-computer simulations for the parametric/subharmonic case

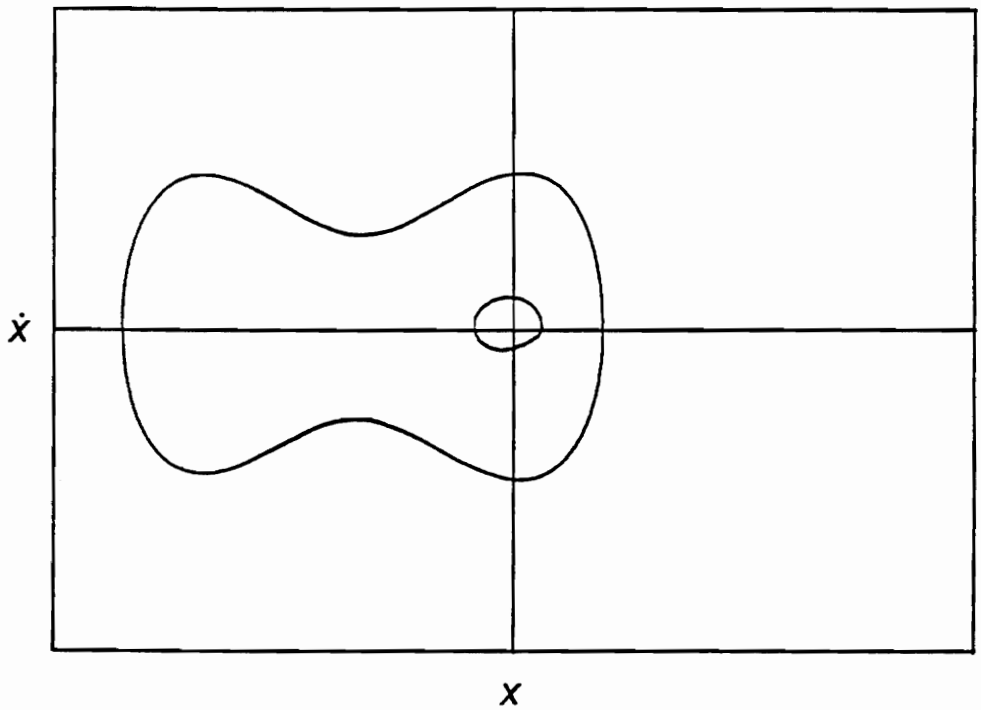

Figure 23. Limit cycles of the disturbance and quenched response from the analog-computer simulations for the primary/superharmonic case

$PS_1 = 0.1$ time scaling
$PS_2 = 0.1$ time scaling
$PS_3 = 0.5$
$PS_4 = 0.1\omega_0^2 = 0.1$

$PS_5 = 0.1\alpha_2 = 0.3$
$PS_6 = 0.1\alpha_3 = 0.2$
$PS_7 = 0.1$
$PS_8 = 0.5$

$PS_9 = 0.6$
$PS_{10} = 10\mu = 0.2$

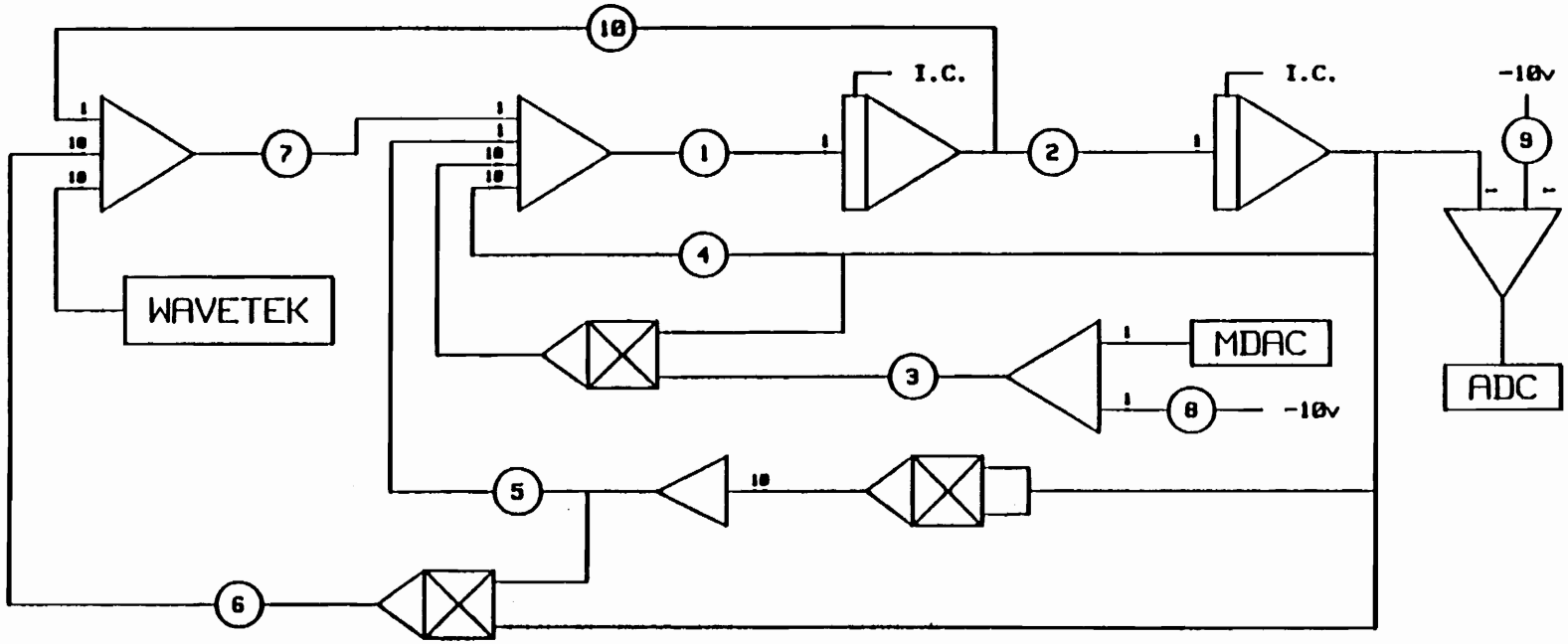

Figure 24. Analog-computer patching diagram for the parametric/subharmonic case

$PS_1 = 0.1$ time scaling
$PS_2 = 0.1$ time scaling
$PS_3 = 0.1$

$PS_5 = 0.1\alpha_2 = 0.3$
$PS_6 = 0.1\alpha_3 = 0.2$
$PS_7 = 0.1$

$PS_8 = 0.5$
$PS_9 = 0.6$
$PS_{10} = 10\mu = 0.2$

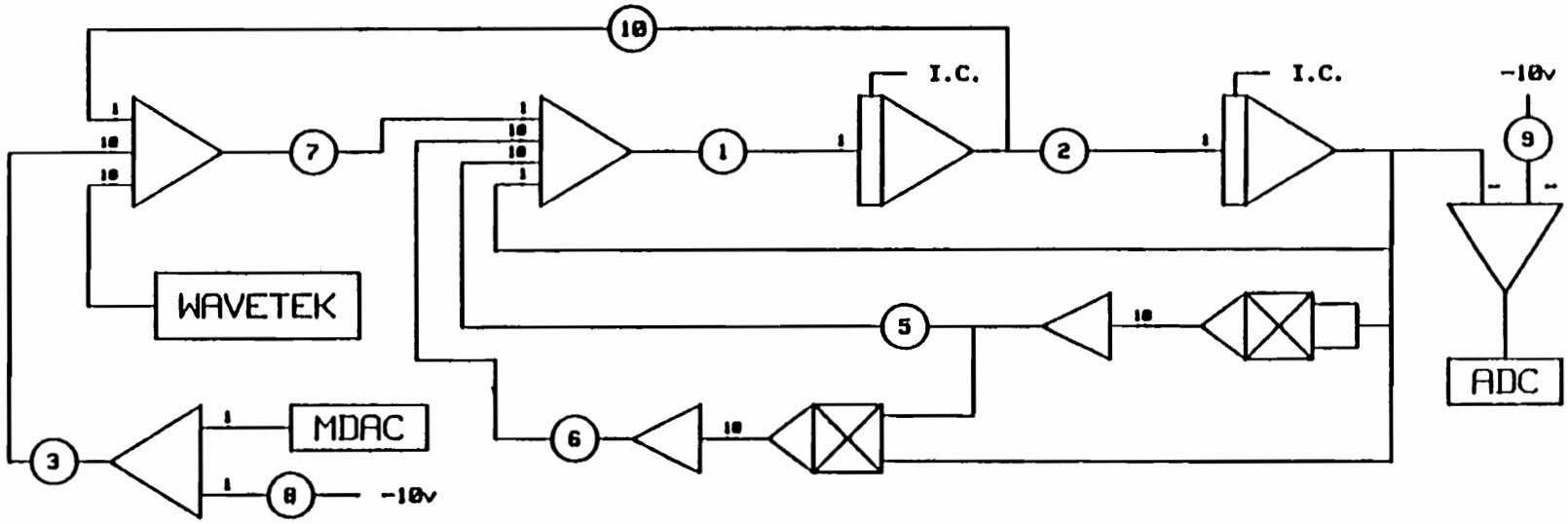

Figure 25. Analog-computer patching diagram for the primary/superharmonic case

CHAPTER 5

CONCLUSIONS

An adaptive quenching algorithm was presented and verified by its implementation on an analog computer. Potential advantages of quenching include a reduction in the required control effort and an alternative to direct disturbance cancellation when the control is unable to enter the process in the same manner as the disturbance. Both quenching and direct disturbance cancellation require a sinusoidal actuator instead of a general force actuator and might prove advantageous in some situations.

For the algorithm to work correctly the filter used must provide estimates of the disturbance and system parameters that are within some neighborhood of the actual parameters for which quenching can occur. After the filter obtains adequate estimates, they need to remain constant over the duration of the disturbance to provide the required constant quenching sinusoid.

In the deterministic case, enhancement (increase) of the response is possible by changing the phase requirement for quenching from $\tau = 0$ to $\tau = \pi$ for the parametric/subharmonic resonant case and from $\tau = \tau_2 - \tau_1$ to $\tau = \pi + \tau_2 - \tau_1$ for the primary/superharmonic resonant case. Let us assume that the modified EKF obtains estimates that satisfy the quenching requirements except for a small steady-state error in the quenching frequency $\Delta\Omega$. Then $\Delta\Omega$ could be modeled as a time-varying error in the phase requirement, resulting in the system cycling through periods of enhancement and quenching. This scenario is prevented by resetting the control sinusoid every T_n seconds. It is the increased range of adequate frequency estimates, as shown in Figures 13-15, that enables adaptive quenching to work.

Quenching requires the parameters of the system and the disturbance to remain constant at least as long as the disturbance is present. Quenching is also dependent on the assumption concerning the relative size of the parameters of the system and disturbance. If either of these two assumptions is violated, disturbance cancellation will have an advantage over quenching. Also quenching results from the interaction of the two resonant excitations and usually requires a longer time to produce a reduction in the system response than direct disturbance cancellation.

In most cases quenching results in the response of the nonlinear system being essentially the linear response. As an alternative to the indirect adaptive method proposed, a model reference adaptive controller (MRAC) might be

formulated using the characteristics of quenching. The true system could be made to follow the response of its linear subsystem to the same disturbance excitation. The problem would be to find the error feedback based update equations for the parameters of the quenching sinusoid.

References

1. Hepburn, J. S. A. and Wonham, W. M., "Error Feedback and Internal Models on Differentiable Manifolds," IEEE Transactions on Automatic Control, Vol. AC-29, No. 5, 1984, pp. 397-403.

2. Francis, B. A. and Wonham, W. M., "The Internal Model Principle of Control Theory," Automatic Control, Vol. 12, No. 5-E, 1976, pp. 457-465.

3. Francis, B. A., Sebakhy, O. A., and Wonham, W. M., "Synthesis of Multivariable Regulators: The Internal Model Principle," Applied Mathematics & Optimization, Vol. 1, No. 1, 1974, pp. 64-86.

4. Chalam, V. V., **Adaptive Control Systems,** Marcel Dekker, Inc., New York, 1987.

5. Elliot, H., and Goodwin, G. C., "Adaptive Implementation of the Internal Model Principle," Tech. Report No. UMASS-ECE-MA 84-1, Dept. of

Electrical and Computer Eng., University of Massachusetts, Amherst, Mass., 1984.

6. Palaniswami, M. and Goodwin, G. C., "An Adaptive Implementation of the Internal Model Principle," Proceedings of the 1987 American Control Conference, June 10-12, Vol. 1-3, 1987, pp. 600-605.

7. Benedetto, M., "Synthesis of an Internal Model for Non-Linear Output Regulation," Int. J. Control, Vol. 45, No. 3, 1987, pp. 1023-1034.

8. Nayfeh, A. H., "Combination Resonances in the Non-linear Response of Bowed Structures to a Harmonic Excitation," J. Sound Vib. Vol. 90, No. 4, 1983, pp. 457-470.

9. Plaut,R. H., HaQuang, N., and Mook, D. T., "Simultaneous Resonances in Non-linear Structural Vibrations under Two-frequency Excitation," J. Sound Vib., Vol. 106, No. 3, 1986, pp. 361-376.

10. Nayfeh, A. H., "Quenching of Primary Resonance by a Superharmonic Resonance," J. Sound Vib., Vol. 92, No. 3, 1984, pp. 363-377.

11. Nayfeh, A. H., "Quenching of a Primary Resonance by a Combination Resonance of the Additive or Difference Type," J. Sound Vib., Vol. 97, No. 1, 1984, pp. 65-73.

12. Nayfeh, A. H., "Interaction of Fundamental Parametric Resonances with Subharmonic Resonances of Order One-Half," J. Sound Vib., Vol. 96, No. 3, 1984, pp. 333-340.

13. Zames, G. and Shneydor, N. A., "Structural Stabilization and Quenching by Dither in Nonlinear Systems," IEEE Transactions on Automatic Control, Vol. AC-22, No. 3, 1977, pp. 352-361.

14. Åström, J. K. and Wittenmark, B., **Computer Controlled Systems,** Prentice-Hall, New York, 1990.

15. VanLandingham, H. F., "Pseudo-Linear Parameter Identification," Conference on Information Science and Systems, Princeton, NJ March 1986.

16. Nayfeh, A. H. and Mook, D. T., **Nonlinear Oscillations,** Wiley-Interscience, New York, 1979.

17. Nayfeh, A. H., **Perturbation Methods,** Wiley-Interscience, New York, 1973.

18. Nayfeh, A. H., **Introduction to Perturbation Techniques,** Wiley-Interscience, New York, 1981.

19. Technical Staff, The Analytic Sciences Corporation, **Applied Optimal Estimation,** edited by A. Gelb, MIT Press, 1974.

20. Jazwinski, A. H., **Stochastic Processes and Filtering Theory,** Academic Press, New York, 1970.

21. Dhingra, J. S., "Estimation of Nonlinear Systems using Jump Matrix Technique," Thesis, Dept. of Electrical Eng., Virginia Tech, Blacksburg, Va. July 1988.

22. Moose, R. L., VanLandingham, H. F., Dhingra, J. S., and Lauzan, T. A., "A Computationally Efficient Technique for State Estimation of Nonlinear Systems," unpublished paper, Dept. of Electrical Eng., VPI

Vita

Bryan D. Heydon was born in Athens, Ohio on May 7, 1966. In 1984 he enrolled at Virginia Tech and received his B.S. in Electrical Engineering in May, 1988. He elected to stay at Virginia Tech and work toward a M.S. in Electrical Engineering specializing in controls and estimation theory. For the past two years he has worked as a Graduate Research Assistant in the Engineering Science & Mechanics Department and has recently completed the requirements for his M.S. degree. He is currently looking for a position in industry and contemplates possibly pursuing a Ph.D. sometime in the future.